

The Development of a Fast Sum-Coincidence
Angular Correlation Gamma Ray Spectrometer and its
Application to Decay Scheme Studies

A Thesis
submitted to the
Faculty of Graduate Studies
University of Manitoba
in partial fulfillment of the
requirements of the degree of

MASTER OF SCIENCE

by

R. Allan Brown

Winnipeg, Canada

April 1964



CONTENTS

List of figures	i
Acknowledgements	iii
Abstract	iv
Section I Introduction	1
The Scintillation Spectrometer	4
The Sum-Coincidence Spectrometer	7
Angular Correlations	12
Section II Apparatus	18
Detectors	22
High Voltage Supply	22
Headers	24
Amplifiers	26
Adder	28
Fast Coincidence	30
Slow Coincidence	35
Voltage Discriminator	35
Single Channel Analyser	37
Section III Results	42
Co ⁶⁰ and Na ²² Sum Spectra	42
Co ⁶⁰ Angular Correlation	45
Removal of Fictitious Cascades	47
Decay of Cs ¹³⁴	50
Bibliography	65

FIGURES

Fig. 1	Block Diagram	19
2	Source Holder and Detector	21
3	Spectrometer Control Panel	21
4	Header Circuit Diagram	23
5	Fast Time Pulse	25
6	Amplifier Circuit Diagram	26
7	Adder Circuit Diagram	27
8	Fast Coincidence Circuit Diagram	30
9	Resolving Time Curve	32
10	Photomultiplier Jitter	33
11	Slow Coincidence Circuit Diagram	35
12	Discriminator Circuit Diagram	37
13	Strobe Unit Circuit Diagram	39
14	Single Channel Analyser Wiring Diagram	41
15	Na ²² Sum Coincidence Spectrum	44
16	Co ⁶⁰ Sum Coincidence Spectrum Sum Window at 2.5 Mev	45
17	Co ⁶⁰ Angular Correlation Curve	47
18	Co ⁶⁰ Sum Coincidence Spectra Sum Window at 1.7 Mev	50
19	Cs ¹³⁴ Decay Scheme a) Nuclear Data Sheets Decay Scheme b) Proposed Decay Scheme	52
20	Cs ¹³⁴ Singles Spectrum	53

Fig. 21	Cs ¹³⁴ Sum Coincidence Spectrum Sum Window at 1970 Kev	54
22	Cs ¹³⁴ Sum Coincidence Spectra Sum Window at 1138 Kev	56
23	Cs ¹³⁴ Sum Coincidence Spectra Sum Window at 1400 Kev	57
24	Cs ¹³⁴ Sum Coincidence Spectra Sum Window at 1640 Kev	59
25	Comparison of Fast and Slow Sum Coincidence Spectra at 1640 kev level	60
26	Cs ¹³⁴ Sum Coincidence Spectra Sum Window at 1773 Kev	62

ACKNOWLEDGEMENTS

The work described in this thesis was carried out at the University of Manitoba from September 1962 to April 1964.

The author wishes to express his sincere thanks to the director of the research - Dr. K. I. Roulston - for his constant interest, encouragement and stimulating discussions, to the Rector of St. Paul's College for allowing him to use the Victoreen Multi-channel analyser and research facilities, and to Dr. S. I. H. Naqvi and Professor W. R. Wall for their constant interest and invaluable assistance in constructing the apparatus.

The financial assistance of the National Research Council of Canada is gratefully acknowledged.

ABSTRACT

The construction of a fast sum-coincidence angular correlation gamma ray spectrometer is described. With the exception of the high voltage power supply the apparatus is completely transistorized.

A method has been developed for removing fictitious cascades, caused by Compton interference, in sum-coincidence spectra, by using in turn, two small crystals ($1\frac{3}{4}$ " diameter x 2") and one small and one large crystal (3" x 3").

The method was tested using the decay of Co^{60} and then applied to the decay of Cs^{134} with the object of elucidating the decay scheme.

Section I

INTRODUCTION

In 1911, Rutherford proposed that the atom consisted of a very small positively charged core, which he called the nucleus, surrounded by moving electrons. Since that time physicists have devoted much effort to learn more about the detailed structure of the nucleus. To this date several models have been proposed (for example, The Liquid Drop Model, The Shell Model, The Optical Model and The Collective Model are some of them.) but no one model has yet been devised which will explain all the phenomena related to the nucleus.

One method of studying a nucleus is to examine the emissions from it. These are generally of three types; alpha (α) particle, beta (β) particle and gamma (γ) radiation. Gamma rays, which are electromagnetic in nature, are believed to come from the nucleus during transitions between the various energy states in which it can exist. Therefore an examination of the gamma rays emitted from a nucleus may give some insight into the structural levels of that nucleus. The study of these nuclear levels is called "Nuclear Spectroscopy".

When a nucleus decays by alpha or beta emission, or by any other nuclear process the daughter nucleus is usually left in an excited state. This new nucleus may then de-excite by several methods, one of the more important of which is by gamma ray emission. When it de-excites by gamma ray emission it can do so by going directly to the ground state or by going to another excited state and then to ground. Thus it is possible for a level to de-excite by several different paths so that a transition between a highly excited state and the ground state may be represented by several gamma rays of different energies. The energy of each of these gamma rays is equal to the difference in energy between the two levels involved.

It is the job of the nuclear spectroscopist to examine these gamma rays and by means of energy considerations, spin consideration and relative intensities, decide upon the structure of the particular nucleus under investigation. It is to be hoped that when enough information has been gathered about the many radioactive nuclei, a suitable nuclear theory may be developed which can explain all the phenomena related to the nucleus.

Spectroscopic investigations of the nucleus began as early as 1911 and for the next thirty years physicists devoted themselves to the laborious task of

gathering data. When isotopes were produced artificially the field of nuclear spectroscopy grew rapidly. During the "forties" a tremendous effort was put into the development of better instruments and techniques in order that data of higher quality might be obtained.

With the advent of the scintillation counter about 1944, nuclear spectroscopy was given one of its most powerful tools - the scintillation spectrometer.

The Scintillation Spectrometer .

A complete description of the scintillation spectrometer can be found in the literature (Roulston 1952, Bell 1955). It is not intended that the following description of a scintillation spectrometer be a thorough one. It is given merely as an outline of how the instrument works.

When a gamma ray passes through matter it loses some or all of its energy. If the gamma ray passes through certain crystals (for example NaI(Tl)) then a light pulse is given off which is proportional to the energy deposited. This light pulse is detected and converted into an electrical pulse by means of a photomultiplier. These pulses are then fed into a linear amplifier to produce pulses of usable size (up to 10v for transistorized equipment and 100v for tube equipment). The pulses are then fed into an analyser which is capable of determining the pulse amplitude distribution or the "scintillation spectrum" of the gamma rays detected.

The scintillation spectrum of a gamma ray source contains distinctive features corresponding with the different interactions between the radiation and the crystal material. These features can generally be identified and permit measurement of gamma ray intensities and energies.

The main features in a spectrum are the Compton distribution, corresponding to Compton interactions, the Gaussian shaped photo-electric "peak" which corresponds with photo-electric interactions, and the pair production "peak" which corresponds with the production of a positron-electron pair. In the pair production process 1.022 Mev of energy is required to create the pair resulting in a peak corresponding with energy absorption by the crystal equal to $E - 1.022$ Mev. When the positron annihilates two 511 Kev gamma rays are emitted resulting in further peaks in the spectrum at $(E - 511)$ Mev and E corresponding to the absorption of one or both annihilation quanta in the crystal.

Other processes also occur with corresponding features in the spectrum. These include peaks at 511 Kev and 1.022 Mev corresponding to the capture of one or both annihilation gamma rays if the source is a positron emitter; a peak at $E(1 + \frac{2E}{.511})^{-1}$ Mev corresponding to the energy of gamma rays back scattered from the materials surrounding the source; escape peaks at $(E - E_K)$ and $(E - E_L)$ provided the energy E is close to E_K and E_L , the binding energy of K and L electrons in the scintillator; a peak corresponding to the x-ray emitted by the daughter nucleus (usually only the K x-ray). While these effects are generally small their existence should be recognised for the accurate interpretation of spectra.

The photopeak of a weak intensity, low energy gamma ray can become completely obscured by the Compton distribution of a stronger, higher energy gamma ray. For this reason, many attempts have been made to construct a spectrometer which will reduce or eliminate the Compton portion of the spectrum (Albert 1953, Roulston 1956, Bell 1954, 1955 and Hoogenboom 1958). A summary of these spectrometers can be found in the literature (Naqvi 1961).

Sum Coincidence Spectrometer

Hoogenboom, in 1958, developed a spectrometer which was particularly suited to measure gamma-gamma coincidence spectra and gamma-gamma angular correlation functions. The main features of this new spectrometer are the following:

- 1) The pulse distribution shows only the "full energy" peak for one specific gamma ray transition.
- 2) The absolute half-widths of the peaks due to coincident gamma rays are, to a first approximation, equal and smaller than the half-widths of the two corresponding full energy peaks in the singles spectrum.
- 3) The detection efficiencies for coincident gamma rays are equal.

The spectrometer works on the principle that the energy involved in a transition from one particular level to the ground state is a constant. Pulses from two crystals are added and sent through a differential discriminator which has a "window" set so that only those pulses from gamma rays which have been totally

absorbed get through. The output from this differential discriminator is used to gate a multi-channel analyser which analyses the pulses from one of the crystals. Thus only full energy peaks of the gamma rays involved in the cascade and a peak due to the absorption of both gamma rays in the one crystal appear in the spectrum.

The resolution of the spectrometer can be calculated if it is assumed that the full energy peaks of the two gamma rays (γ_a and γ_b with energies E_a and E_b) have a Gaussian shape with half-widths Γ_a and Γ_b and that the sum peak is also Gaussian with a half-width Γ_s at energy $E_s = E_a + E_b$. Under these conditions it can be shown* that the half-width of the peak in the sum spectrum corresponding to γ_a is

$$\Gamma_{sa} = \frac{\Gamma_a \sqrt{\Gamma_b^2 + \Gamma_s^2}}{\Gamma} \quad \text{--- (1)}$$

where $\Gamma^2 = \Gamma_a^2 + \Gamma_b^2 + \Gamma_s^2$.

Inspecting this formula it can be seen that the peak in the sum spectrum is narrower than the corresponding peak in the single spectrum. If the sum peak is made much narrower than Γ_a or Γ_b then

$$\Gamma_{sa} = \frac{\Gamma_a \Gamma_b}{\Gamma} \quad \text{--- (2)}$$

*

Naqvi (1961)

This means that the peaks in a sum coincidence spectrum have the same half-widths to a first approximation.

The efficiency ϵ_{sa} of detecting γ_a in the sum spectrum can be expressed in terms of the full energy efficiencies of detecting γ_a and γ_b in the singles spectrum. The efficiency ϵ_{sa} is given as

$$\epsilon_{sa} = 2 \sqrt{\frac{\ln 2}{\pi}} \epsilon_a \epsilon_b \frac{\sqrt{s}}{\Gamma} \quad \text{--- (3)}$$

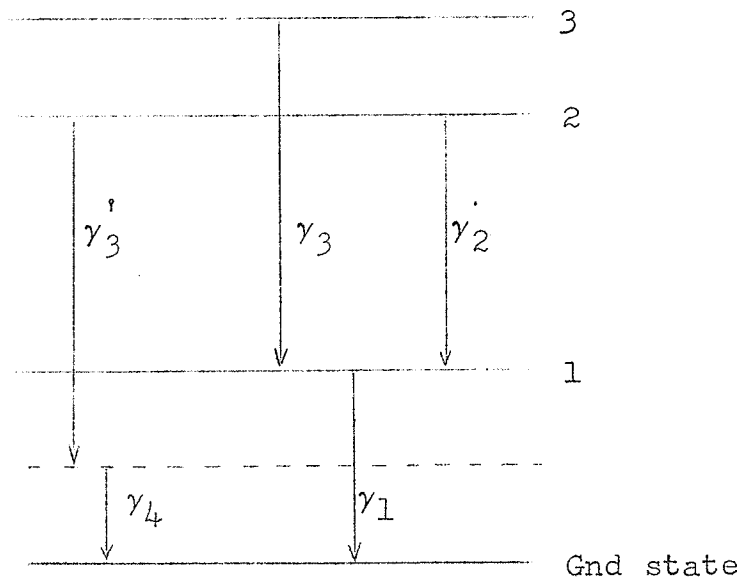
Provided the crystals being used in the experiment are of the same size, since the above expression for ϵ_{sa} is symmetrical with respect to the indices a and b, then the area under the peaks in the sum spectrum corresponding to γ_a and γ_b have to be equal.

In comparing equations (2) and (3) it should be noted that a compromise between good resolution and good efficiency has to be effected in regard to the setting of the sum "window" width. Hoogenboom has suggested that a good compromise is to make Γ_s of the order of the smaller of Γ_a and Γ_b .

The efficiency of detection of the cross-over equals $\epsilon_{sab} = \frac{\sqrt{s}}{\Gamma_{ab}} \epsilon_{ab}$, where Γ_{ab} and ϵ_{ab} are the half-width and efficiency of detecting the cross-over transition in the singles spectrum. In order to calculate the intensity of this cross-over transition a correction

must be made for background and for the contribution from both gamma rays depositing their energy in the same crystal. If the geometry is symmetric, then this correction amounts to one half the intensity of all other peaks in the spectrum.

In the foregoing, it has been assumed that only full energy peaks give rise to peaks in the sum spectrum. This is the case only when the sum peak corresponds to the highest energy level in the nucleus. If the sum window is set at any intermediate level then the coincident gamma rays from that level will appear in the spectrum, but there can also be a contribution from Compton events of higher energy transitions.



For example, consider a scheme such as that shown in the accompanying figure with the sum window set at the energy corresponding to level two. The sum spectrum will show peaks corresponding to γ_1 and γ_2 . However peaks could also appear in the spectrum from γ_3 adding with Compton events from γ_1 giving the impression that there should be another level in the scheme (dotted in the figure) with a gamma ray γ_4 between it and the ground state.

Recently in a paper by Schriber and Hogg (Schriber 1963), a method has been developed for calculating the amount of Compton interference in the spectrum and subtracting it. It is the object of this thesis to construct a sum coincidence spectrometer and to develop an experimental method of eliminating, or reducing the Compton interference.

Angular Correlations

The study of angular correlations of successive gamma rays in a cascade began in 1940. The first theory on directional correlations was proposed by Hamilton (Hamilton 1940) in that year and for the next few years many people tried to obtain results which would agree with this theory. They were however unsuccessful, and even the attempts of Goertzel (Goertzel 1946) in a theoretical paper on the effects of the influence of extra nuclear fields on the directional correlation could not bring these results into line. The first successful experiments on directional correlation were performed by Brady and Deutsch in 1947 (Brady 1947) using Geiger counters. They showed that it was not the theory that was at fault but the experimental techniques.

In 1948 Brady and Deutsch (Brady 1948) introduced scintillation counters into directional correlation work. These greatly reduced the time required for a correlation and since that date the literature has contained several hundred papers on the subject of directional correlations. There have been many theoretical papers written on the subject, with different degrees of sophistication ranging from Hamilton's treatment of the "Naive Theory" (see Siegbahn 1955) to treatments involving Racah algebra.

The reader is referred to the literature for a detailed description of the theory. It will suffice to give here a brief description of Hamilton's treatment with some comments regarding its limitations and subsequent improvements.

The "Naive" Theory of Angular Correlation

The probability of emission of a gamma ray depends upon the angle between the direction of the nuclear spin axis and the direction of emission. Since in a radioactive source the nuclei are randomly orientated, an isotropic distribution is observed. An anisotropic distribution will be observed only from a source which does not have randomly orientated nuclei. This can be detected by placing the source in a magnetic field or by measuring the distribution of gamma rays with respect to other gamma rays emitted in a known direction. The nuclei emitting gamma rays in a fixed direction have a non isotropic spin distribution. The directional distributions of the other gamma rays from these nuclei can be measured relative to this orientation.

Consider first of all a single gamma ray transition with angular momentum \underline{L} between the nuclear levels B and C with spins I_b and I_c . Let the gamma ray

be characterized by the quantum numbers L and M and the levels by $I_b m_b$ and $I_c m_c$. Then the following relations hold: $\underline{I}_b = \underline{I}_c + \underline{L}$ $m_b = m_c + M$ where $\underline{L}^2 = L(L+1)\hbar^2$, $L_z = M\hbar$.

Each component $m_b \rightarrow m_c$ between specified magnetic sub levels has a directional distribution function $F_L^M(\theta)$ where θ is the angle between the gamma ray and the z axis. In atomic spectroscopy the individual components of the line $B \rightarrow C$ can be resolved but in nuclear spectroscopy they cannot be. In order to calculate the directional distribution of the line it is necessary to know the relative population $P(m_b)$ of each sub level m_b and the transition probability $G(m_b m_c)$ for each component $m_b \rightarrow m_c$. Then

$$F_L^M(\theta) \sim \sum_{m_b m_c} P(m_b) G(m_b m_c) F_L^M(\theta)$$

is the directional distribution for the unresolved line.

The absolute transition probability for a component $m_b \rightarrow m_c$ can be written as a product of a "nuclear" factor and a "geometrical" factor. It can be shown that the relative transition probability for a transition from $m_b \rightarrow m_c$ is given by

$$G(m_b m_c) = (I_c L m_c M | I_b m_b)^2$$

where the right hand side is a Clebsch-Gordan coefficient.

In order to calculate the relative populations it is necessary to know how the level B was created. Consider another level A decaying to B and then to C. If the direction of the gamma ray emitted from level A is taken as the Z axis the calculations will be greatly simplified and a directional correlation between the two successive gamma rays will be obtained. If all the m_a states are equally populated then

$$P(m_b) \sim \sum_{m_a} G(m_a m_b) F_{L_1}^{M_1} (\theta = 0) \text{ where}$$

$M_1 = m_a + m_b$. (for short-lived intermediate level)

This special choice of Z axis has also restricted the possible values of $F_{L_1}^{M_1}$ to $F_{L_1}^{\pm 1}$ since a gamma ray emitted in a specific direction can carry only the angular momentum $+\hbar$ or $-\hbar$.

Thus the directional correlation function $W(\theta)$ becomes

$$W(\theta) \sim \sum_{m_b m_c m_a} (I_b L_1 m_b \pm 1 | I_a m_a)^2 F_{L_1}^{\pm 1}(0) (I_c L_2 m_c M_2 | I_b m_b)^2 F_{L_2}^{M_2}(\theta)$$

Hamilton derived this equation using second order damping theory and evaluated it for possible cascades involving pure dipole and quadrupole gamma rays. He used an expansion

$$W(\theta) = 1 + a_2 \cos^2 \theta + a_4 \cos^4 \theta$$

and gave explicit forms for a_2 and a_4 . These calculations were, however, very tedious and extremely difficult to transform to higher multipolarities.

The next improvement in the theory of angular correlations came from Yang (Yang 1948) and Fierz (Fierz 1949) using group theory methods. Yang proved some general statements about $W(\theta)$ and Fierz calculated the expressions for the angular correlation functions of gamma rays and conversion electrons but could not give closed formulae.

The next improvement came from Gardner (Gardner 1949) who expressed the function $W(\theta)$ as

$$W(\theta) = 1 + \sum_{k=1}^{k_m} A_{2k} P_{2k}(\cos \theta)$$

where $P_{2k}(\cos \theta)$ are Legendre Polynomials. The coefficients A_{2k} were now in closed form and could be calculated since they were the product of five Clebsch-Gordan coefficients. The calculations of Gardner were restricted to conversion electrons, but Racah (Racah 1951), Lloyd (Lloyd 1950, 1951) and Alder (Alder 1951, 1952) extended them to cover different types of radiation, i.e., alpha-gamma and beta-gamma correlations as well as gamma-gamma correlations involving different multipolarity gamma rays.

The correlation function $W(\theta)$ can be written as

$$W(\theta) = 1 + A_2 P_2(\cos \theta) + \dots + A_{\gamma_{\max}} P_{\gamma_{\max}}(\cos \theta)$$

where the highest order in the expansion is determined by the selection rule

$$\gamma_{\max} = \text{Min} (2I_b, 2L_1, 2L_2).$$

The calculation of the coefficients is relatively simple since they are a product of two functions, each of which depends only on one transition of the cascade.

$$A_{\gamma} = F_{\gamma}(L_1 I_a I_b) F_{\gamma}(L_2 I_c I_b)$$

These coefficients have been calculated by Biedenharn and Rose (Biedenharn 1953) and can be found in a report by Ferentz and Rosenzweig (Ferentz 1954).

Section II

APPARATUS

Before embarking upon a description of the individual units in the apparatus, a brief description of the operation of a sum coincidence spectrometer will be given. The apparatus described here (see Fig. 1) differs from that described by Hoogenboom (Hoogenboom 1958) in that it employs the fast coincidence technique in addition to the sum coincidence.

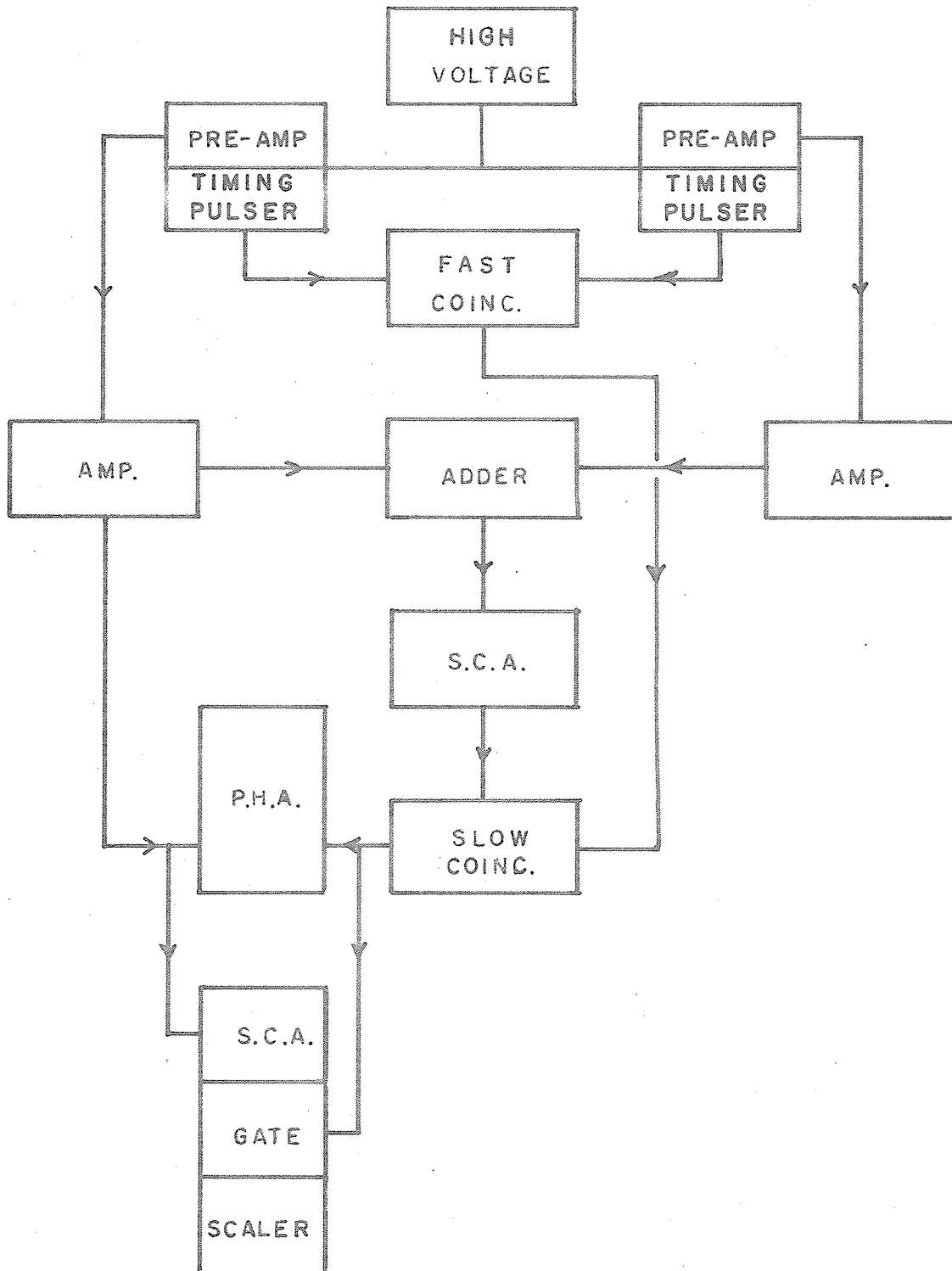
The gamma rays from the source under investigation are detected by means of two scintillation counters. The base unit (the header) of each photomultiplier contains two circuits. One of these, a timing pulse shaper, produces a short fast rising pulse which is fed to the fast coincidence unit, the other, a slower rising linear pulse used for analysis. Thus if two gamma rays are detected by the detectors within the resolving time of the fast coincidence unit, a pulse is generated by this circuit. The preamplifier outputs are fed through linear amplifiers, with equal energy calibration, to an adding circuit. The output from the adder is connected to a single channel analyser so adjusted that only pulses of a certain height

FIGURE 1

SCHEMATIC DIAGRAM OF THE SUM
COINCIDENCE SPECTROMETER

SUM COINCIDENCE SPECTROMETER

BLOCK SCHEMATIC



are passed. Both the fast coincidence and the single channel analyser outputs are fed to a slow coincidence unit which produces a gating pulse for the multi-channel analyser if the inputs are coincident. While the gate is open the delayed pulses from one of the amplifiers are analysed, giving a spectrum showing only those gamma rays which are in coincidence with others and which meet the requirements of the sum window.

The system used by Hoogenboom did not incorporate a fast coincidence unit the multi-channel analyser being gated directly from the differential discriminator output. While this allows the desired gamma rays to be analysed, the spectrum also contains a peak corresponding to the sum energy. This peak arises from two causes:

a) both of the cascading gamma rays could be absorbed in the same crystal, giving rise to a pulse which would get through the sum window.

b) cosmic rays losing an amount of energy equal to that registered by the sum window.

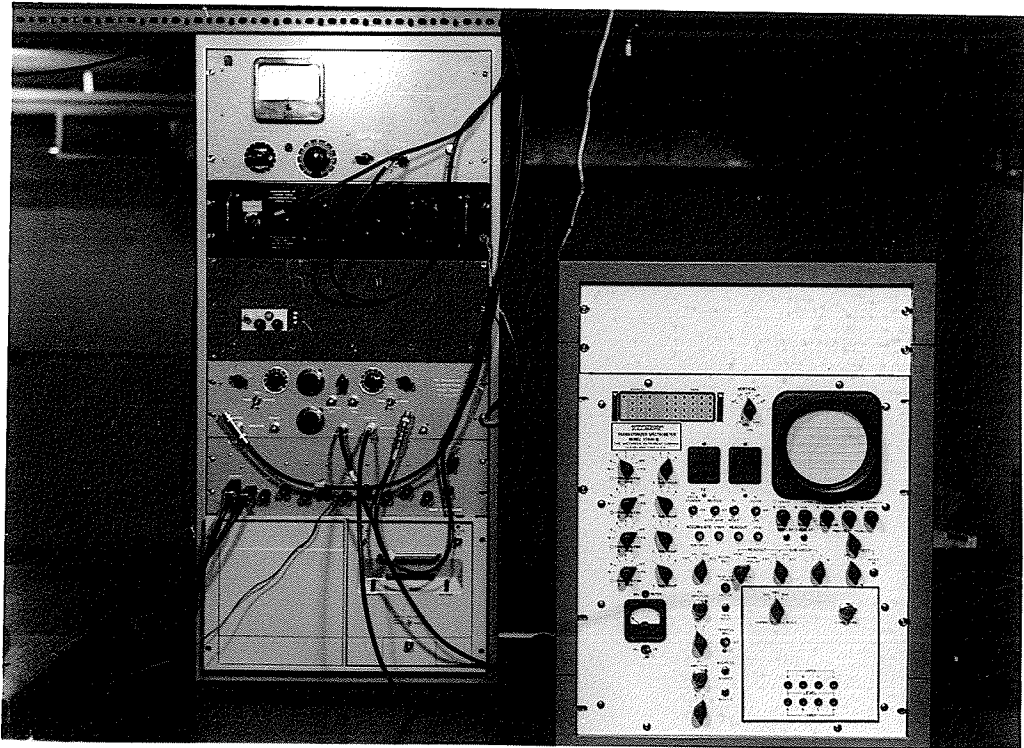
The introduction of a fast coincidence circuit removes the sum peak and also significantly reduces the number of chance coincidences. If the accidental coincidences were not too serious with the original system then the fast

FIGURE 2

SOURCE HOLDER AND DETECTORS

FIGURE 3

SPECTROMETER CONTROL PANEL



coincidence allows the use of stronger sources thus reducing the time required for data accumulation.

A photograph of the source holder and detector assembly is shown in Fig. 2 while Fig. 3 shows a photograph of the electronic equipment. A description of the individual units now follows:

Detectors:

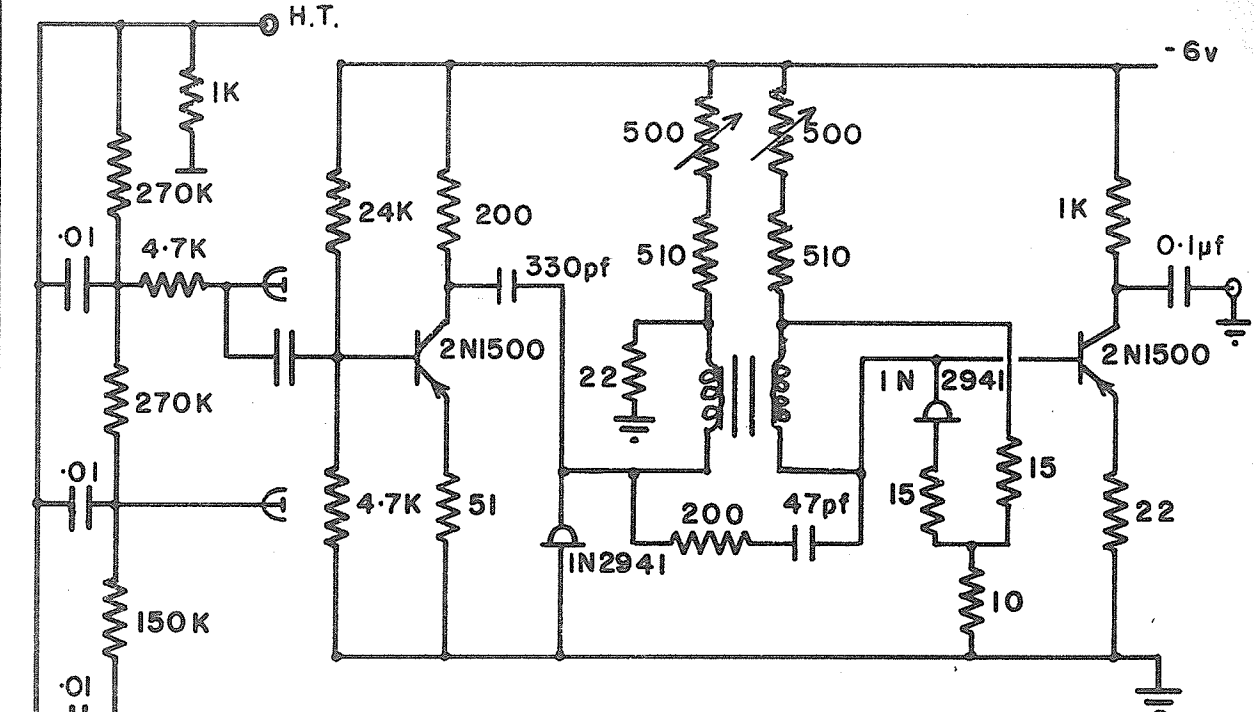
The gamma rays were detected by means of three Harshaw (NaI(Tl)) integral line detectors. Two of these have $1\frac{3}{4}$ " diameter x 2" crystals optically coupled to 2" R.C.A. photomultipliers type 8053 while the third has a 3" x 3" crystal optically coupled to a 3" photomultiplier type 8054. The small crystals have a resolution of 8.3% and 9.0% respectively at 661 Kev and the 3" x 3" crystal has a 7.8% resolution at the same energy. All three units have ten stage photomultipliers. The "fast" pulse for the timing pulse shaper was developed across a 4.7K resistor in the 10th dynode and the "slow" pulse across a 1 Meg ohm resistor in the 7th dynode. Both pulses are therefore positive.

High Voltage Supply:

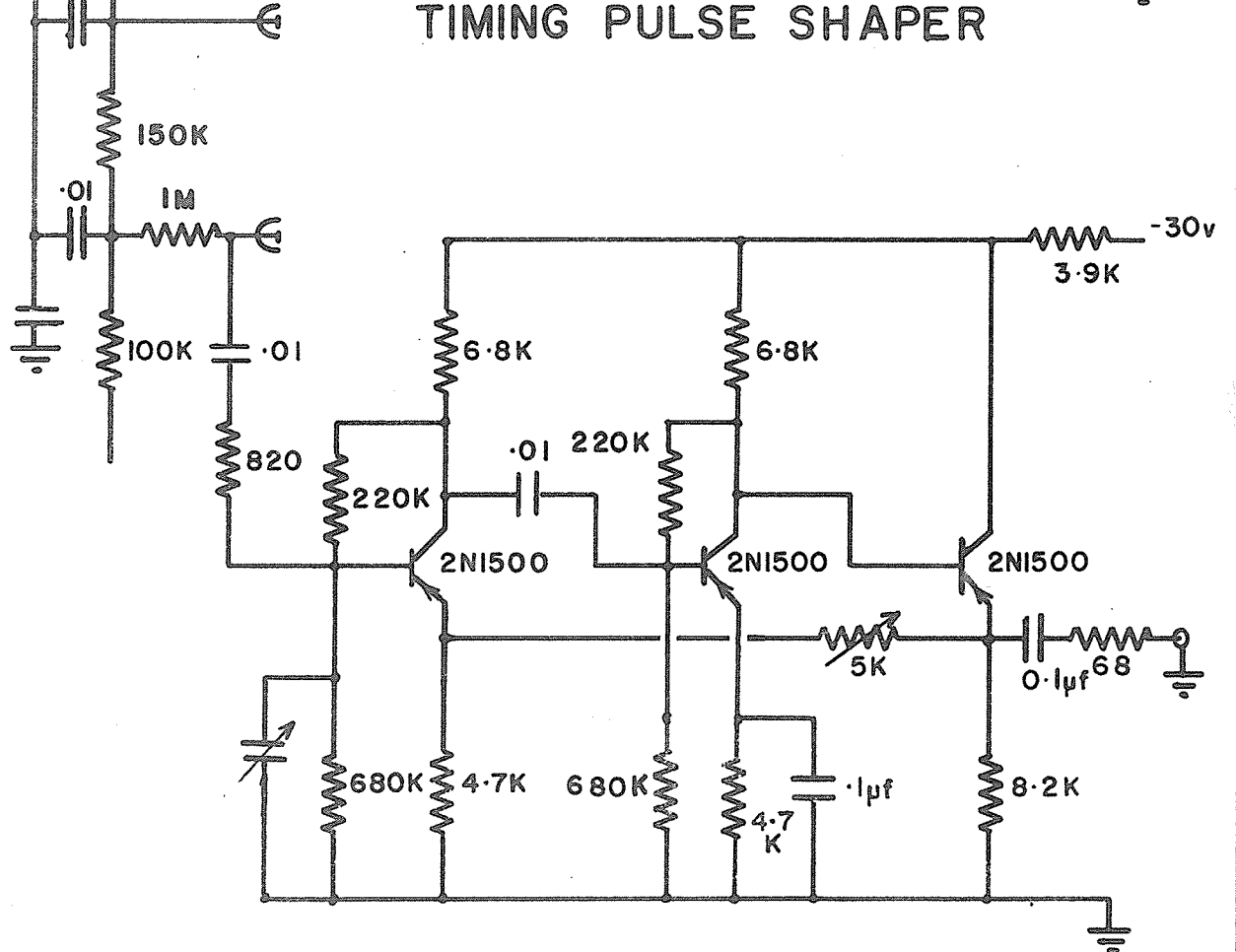
The high voltage power supply is essentially a Hamner unit with certain modifications made to improve the stability. All resistors are now either wire wound

FIGURE 4
HEADER CIRCUIT DIAGRAM

HEADER



TIMING PULSE SHAPER



PRE-AMP

or 1% stabilized carbon in order to reduce the effect of temperature variations. The stability was checked against a temperature stable Zener reference diode and was found to be better than 1 part in 10,000 per day.

Headers:

The header contains two circuits, a timing pulse shaper and a linear preamplifier (see Fig. 4 for circuit diagrams).

The timing pulse shaper is basically the design of Birk et al (Birk 1963). The tunnel diodes in the present circuit are 5 mA Germanium type 1N2941 with the load resistors adjusted accordingly. The input impedance was adjusted to match the photomultipliers. The output transistor is used to invert and amplify the negative pulse from the second tunnel diode. Another modification made here is the introduction of coupling between the inductors of the two stages. They are coupled by means of a fast ferrite core which produces a better transfer of signal from the first tunnel diode to the second than by resistive coupling alone. The circuit can be triggered on 5 mV pulses.

Fig. 5 shows a photograph of the "fast" pulse as displayed on the screen of a Tektronix Type 517 Cathode Ray Oscilloscope which has an intrinsic rise

FIGURE 5

FAST TIME PULSE

TIME SCALE: 10 nsec/cm

AMPLITUDE SCALE: $\frac{1}{2}$ volt/cm

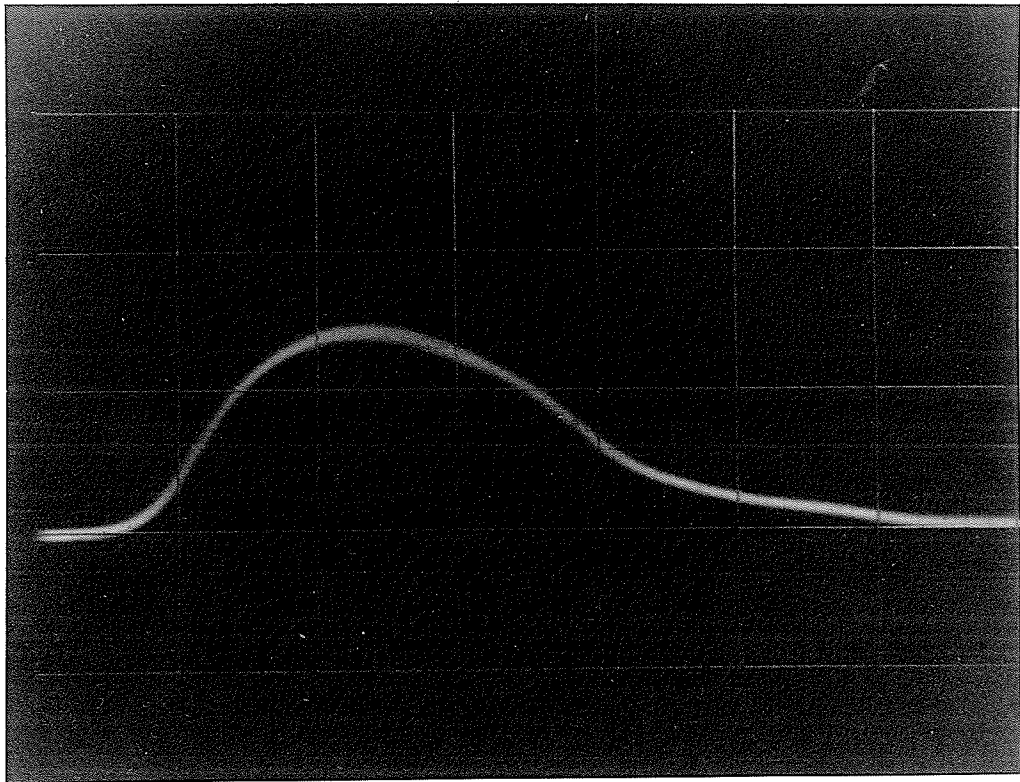
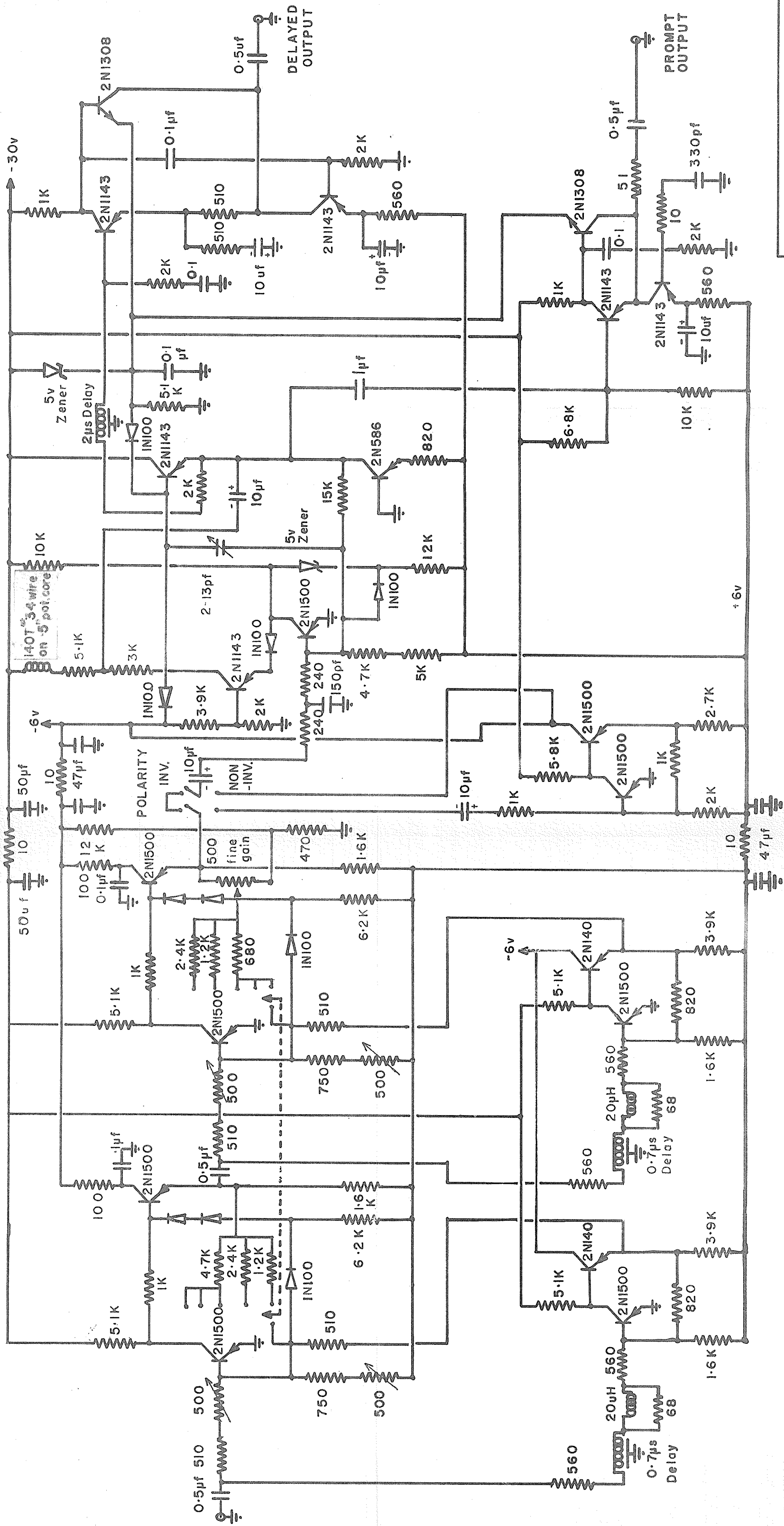


FIGURE 6

AMPLIFIER CIRCUIT DIAGRAM



LINEAR AMPLIFIER

time of 7 nsec. The time base was set at 10 nsec per cm showing that the rise time of the pulse is within the rise time of the oscilloscope and has an overall length of 30 nsec.

The linear preamplifier was designed in this laboratory. It consists of three stages each of which uses fast 2N1500 PNP transistors. The first stage amplifies the incoming pulse, the second stage inverts it, since a positive output is required, and the third stage acts as an emitter follower. The bias for the transistors is developed from the current drawn by them and should normally be dependent upon counting rate. In order to counteract this, extensive use has been made of bias stabilization by large negative current feedback making this effect negligible. Pulses corresponding to an energy of 1.33 Mev are 30 mv high with a rise time of .2 μ secs. (See Fig. 4 for circuit diagram)

Amplifiers:

Amplifiers designed by Chase and Svelto at Brookhaven (Chase 1961) were used for these experiments. (See Fig. 6 for circuit diagram.) They produce a symmetrical double delay line differentiated pulse up to 10 volts high with an overall length of 1.8 μ secs. Both a prompt signal and one delayed by 2 μ secs are available.

FIGURE 7

ADDER CIRCUIT DIAGRAM

*

1% TOLERANCE

Delay line clipping is most commonly accomplished with a short -circuited delay line driven from a source with output impedance equal to the characteristic impedance of the delay line. If amplifiers are subjected to high overload conditions, then high quality delay lines must be used and the termination must be carefully adjusted so that reflections do not produce spurious pulses. Chase and Svelto perform the clipping by means of a relatively cheap helically wound delay line terminated at both ends. This reduces the spurious signals by more than an order of magnitude. The amplifiers can stand an input pulse 400 times overload before producing a spurious output and can handle counting rates of 200,000 per sec.

With the exception of the fast coincidence unit the remainder of the equipment constructed for this project was designed by Goulding and McNaught at Chalk River (Goulding 1960). A description of their equipment and its subsequent modifications follows.

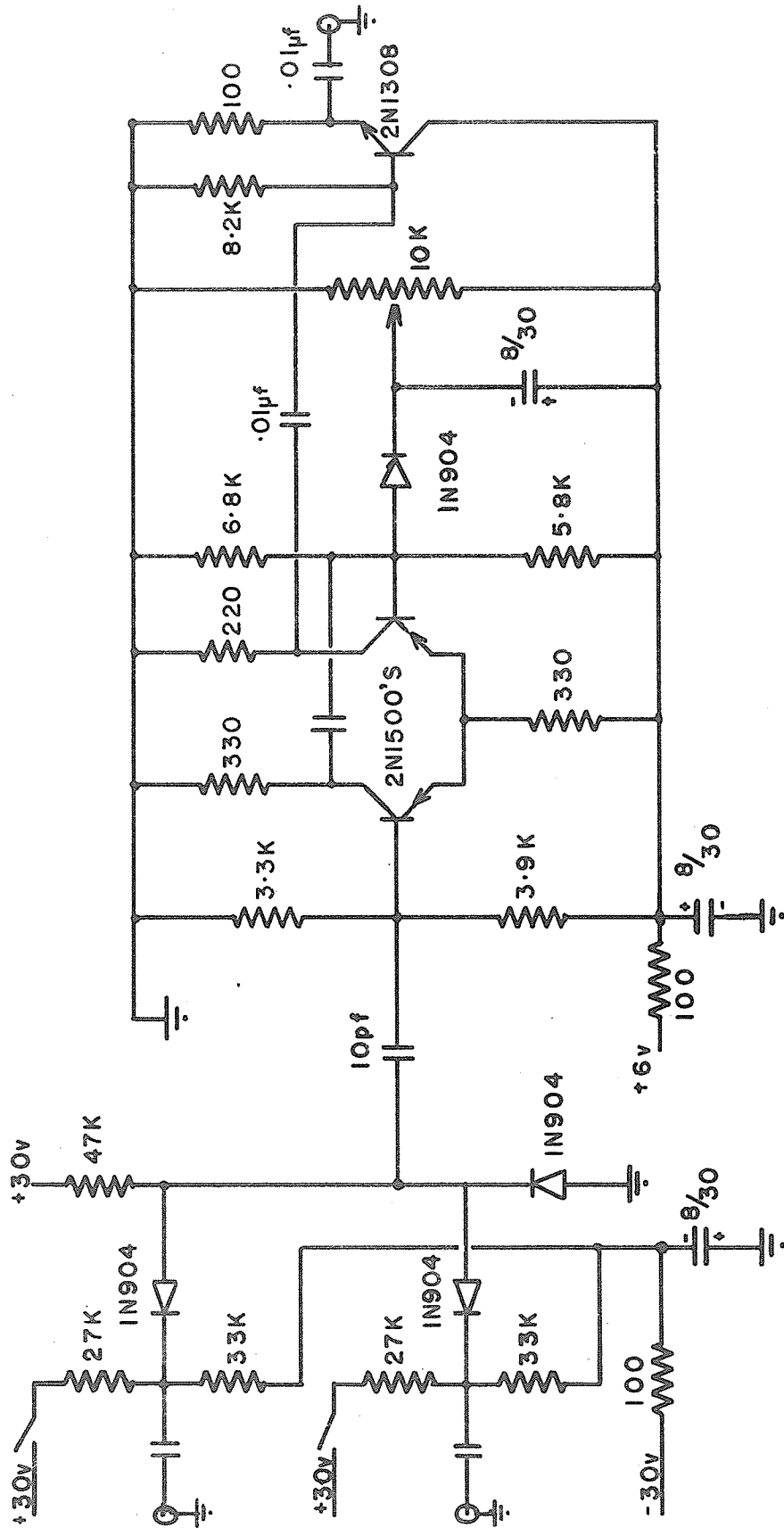
Adder:

The adder amplifier (Fig. 7) is capable of adding two inputs up to ± 4 v each or of providing a 2 times gain in a circuit when the direct input is used. The input transistors constitute a DC feedback amplifier with the base of a 2N1500 acting as a virtual ground to

FIGURE 3

FAST COINCIDENCE CIRCUIT DIAGRAM

FAST COINCIDENCE



provide an adding point for the inputs. The output stage is the transistorized version of the White cathode follower and can drive a signal of up to +6v into a 100 ohm cable,

Fast Coincidence:

The fast coincidence unit was designed by Fraser and Tomlinson (Fraser 1962) at Chalk River (see Fig. 8 for circuit diagram). Extensive use has been made of fast 1N904 diodes and fast 2N1500 PNP switching transistors. When used as a coincidence unit the 27K resistors attached to the inputs are disconnected from the +30 v line. When connected to the 30v line a negative pulse will produce an anticoincidence. When two pulses are coincident the third 1N904 stops conducting, thus producing a positive pulse which is fed to the fast discriminator. The discriminator is of the common emitter type - somewhat similar to the old Schmitt trigger circuit. The triggering level is controlled by varying the base voltage of the second transistor. A 2 volt output pulse is developed and coupled out through a fast N.P.N. emitter follower.

The resolving time of the circuit was calculated by two different methods. Delays were inserted into one input with respect to the other and the coincidence counting rate was plotted against delay as shown in Fig. 9.

FIGURE 9
RESOLVING TIME CURVE

RESOLVING TIME

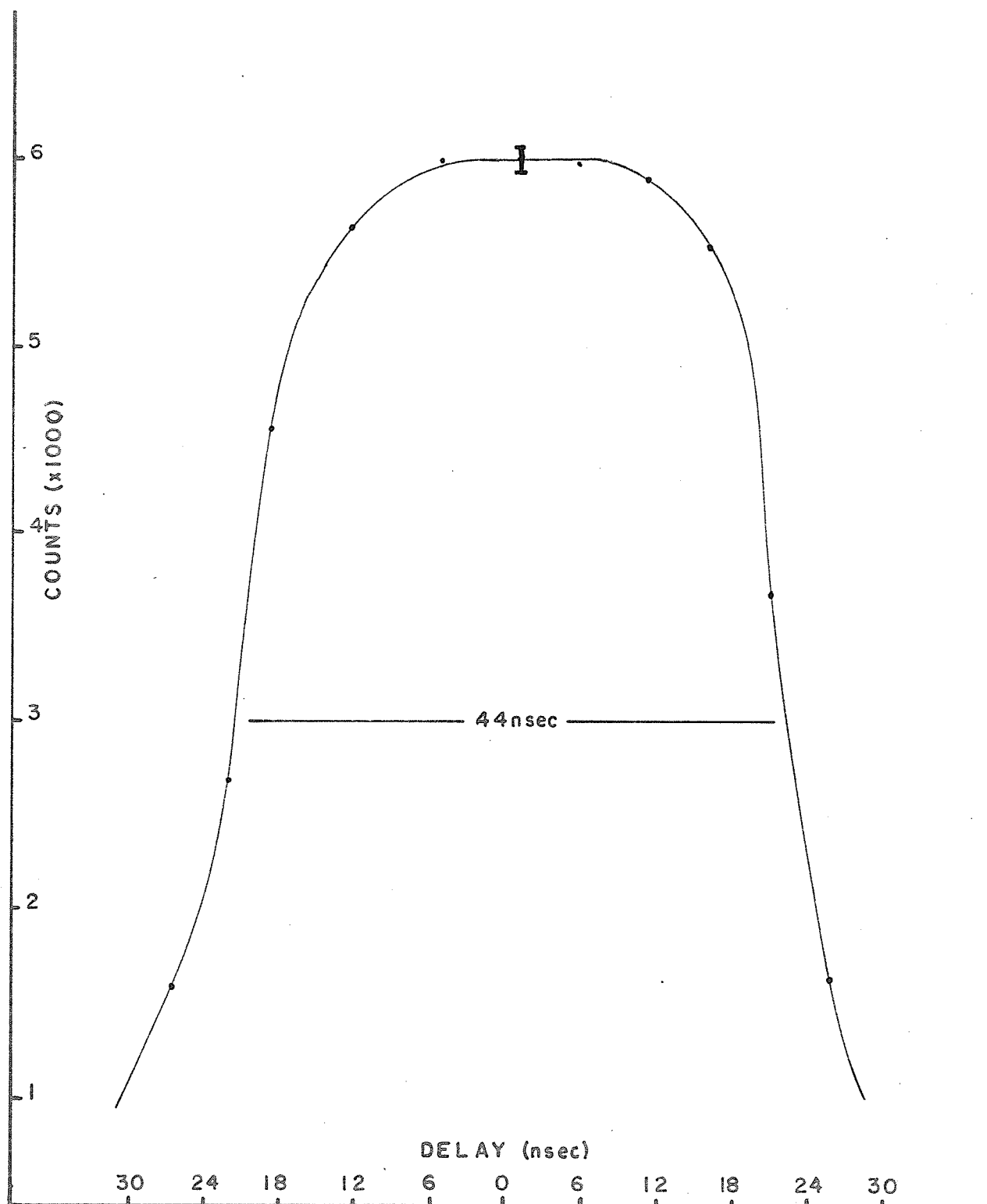
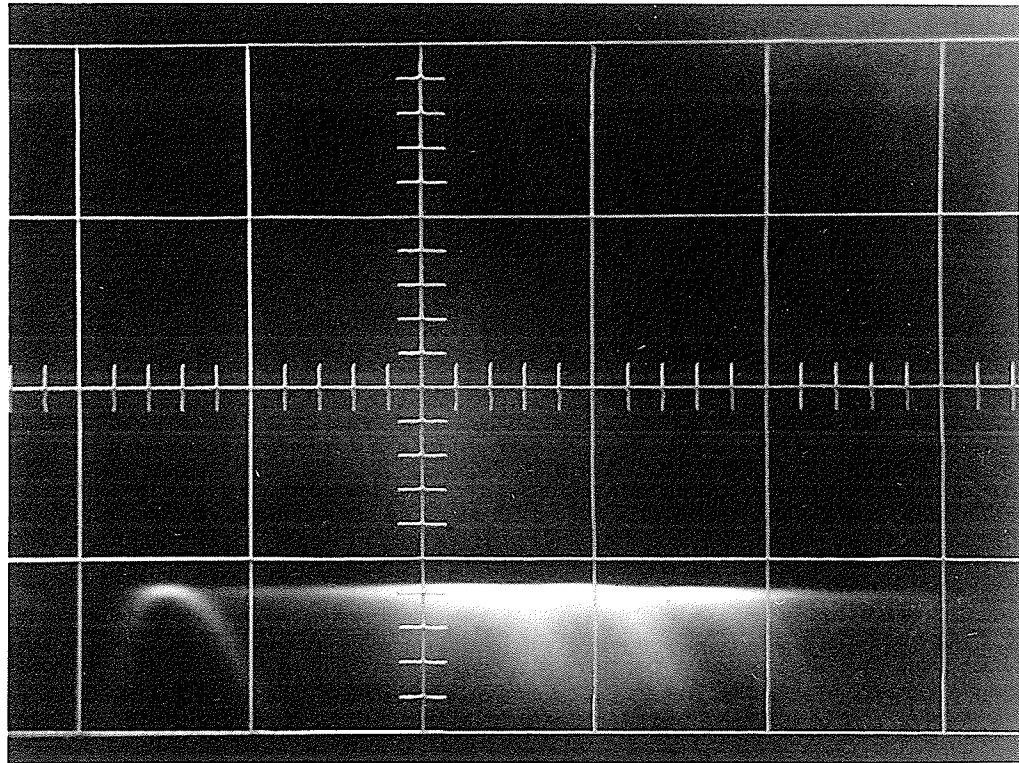


FIGURE 10

PHOTOMULTIPLIER JITTER

TIME SCALE: 20 nsec/cm



The pulses used for this measurement came from the timing pulse shaper and were produced by means of a Co^{60} source. The F.W.H.M. was found to be 44 nsec giving a resolving time, τ , of 22 nsec.

The resolving time was also calculated by the chance coincidence method. Each photomultiplier looked at a source, well shielded from the other by lead, and the number of chance coincidences was noted. The resolving time was then calculated using the relation

$$N_{CH} = 2\tau N_1 N_2 \quad \text{where}$$

N_{CH} = number of coincidences per sec,

N_1 & N_2 = number of counts per sec detected by counters 1 & 2,

τ = resolving time in secs.

Several trials were made giving an average value of $\tau = 26\text{nsec}$ which compares favourably with the previous calculation.

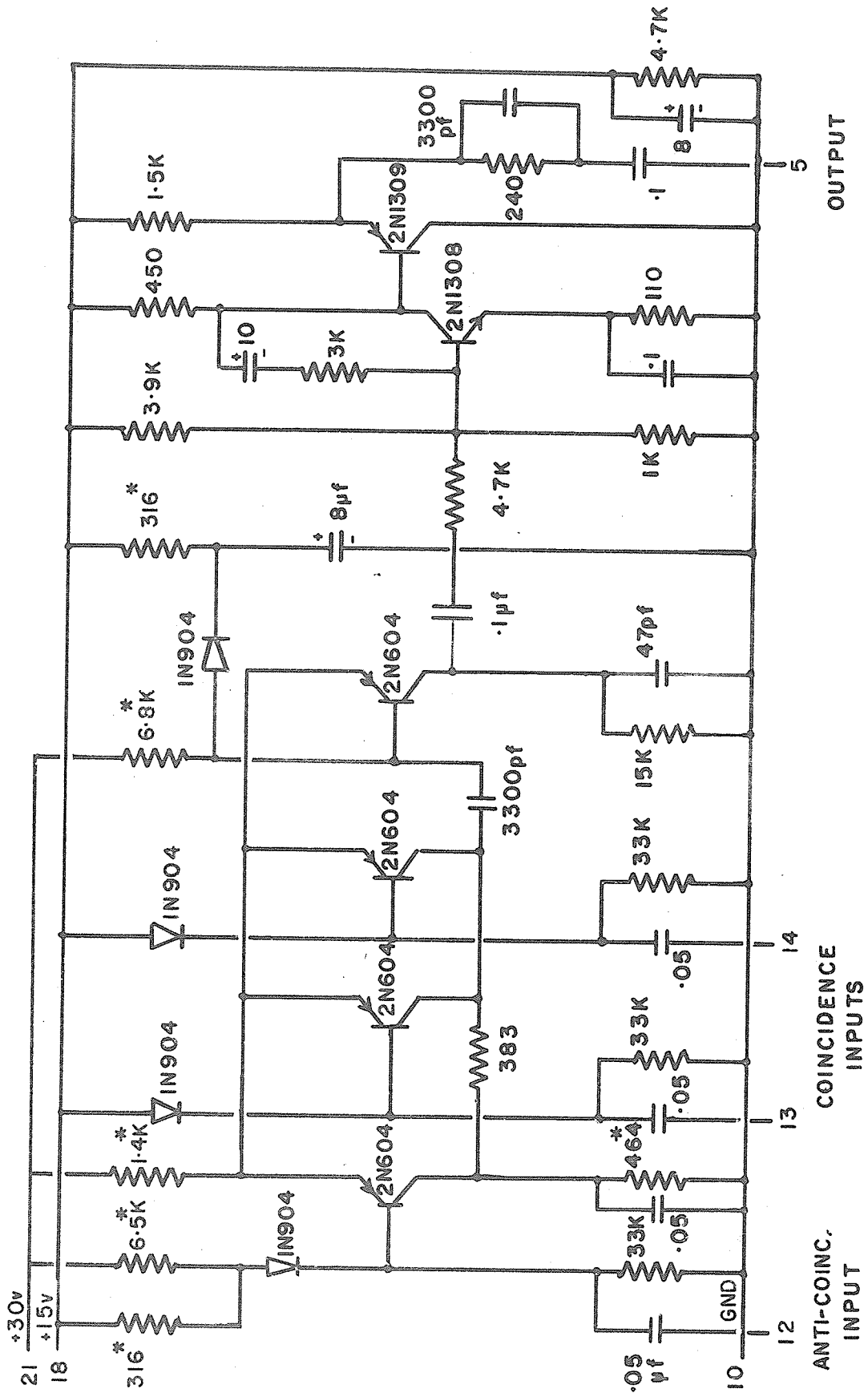
No attempt was made to reduce the resolving time by shortening the "fast" pulses as this resolving time is short enough to reduce the accidental coincidences substantially from the slow unit, and yet long enough to cover the jitter due to transit time spread in the photomultipliers. Fig. 10 shows the jitter in transit time of the photomultipliers photographed on a type 581 Tektronix C.R.O., which was triggered by the output

FIGURE 11

SLOW COINCIDENCE CIRCUIT DIAGRAM

ALL RESISTORS ARE GIVEN IN OHMS

SLOW COINCIDENCE



of one timing pulse shaper while the other "fast" output was fed to the Y axis input. The time base is 20 nsecs per cm.

Slow Coincidence:

The circuit accepts two +1v inputs which, if coincident for about 20 nsecs, produce a positive output pulse (+10 mA) 2 μ secs wide. A +1v anticoincidence pulse, if applied to pin 12 for the entire time the other pulses are in coincidence, prevents an output being generated. The size of the input pulses can be varied from 0.6v to 1.5v with no effect in the output.

The circuit diagram shown (Fig. 11) differs from the original in that it has an inverter and emitter follower after the normal output. These modifications were necessary since the Victoreen multichannel analyser requires a -5v pulse for gating purposes.

Voltage Discriminator:

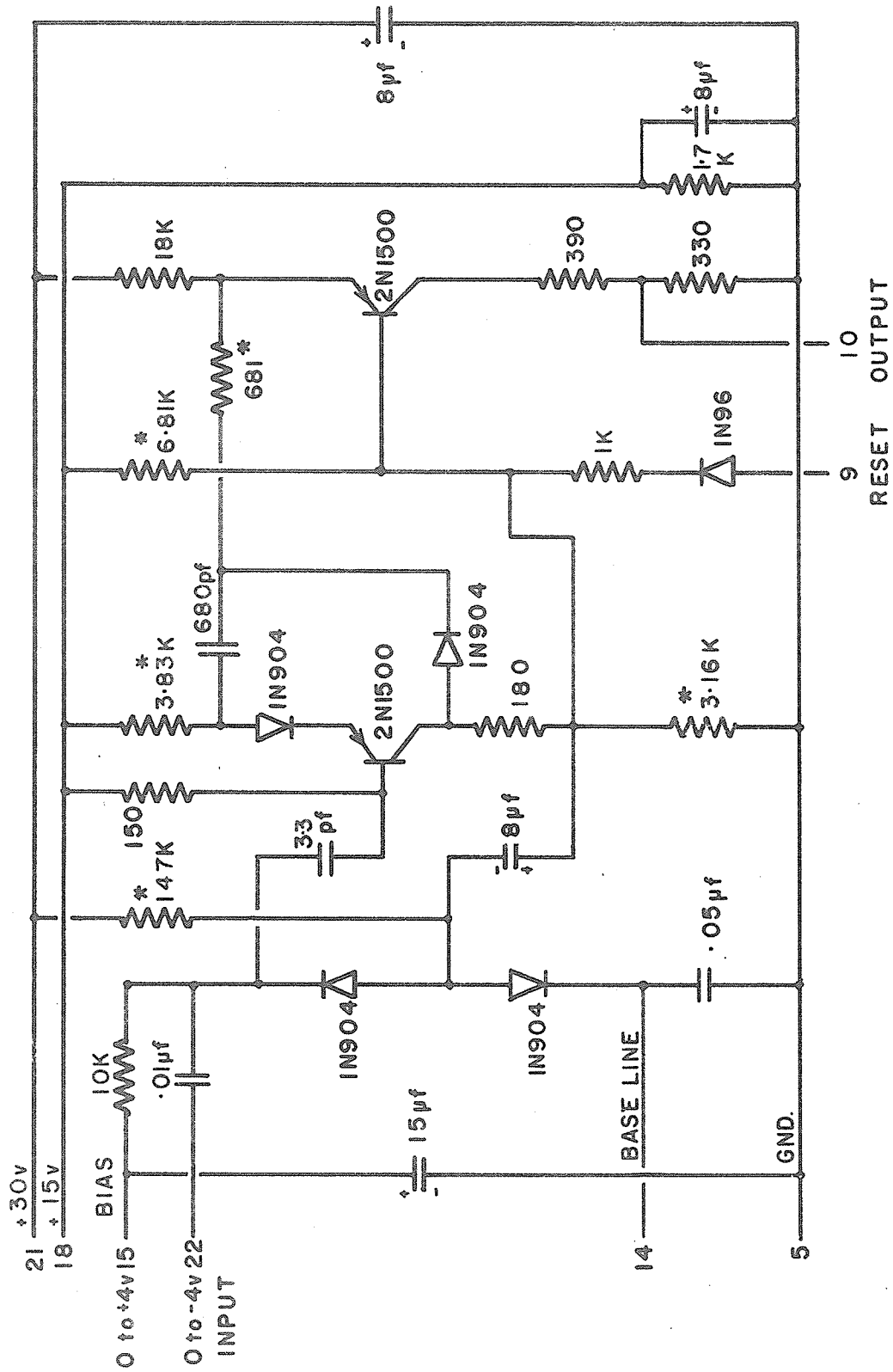
The use of low level pulses common to transistorized equipment demands a high degree of stability in a voltage discriminator. The necessary threshold sensitivity cannot be achieved by a single semiconductor diode since the voltage drop in such a diode, for a constant current through it, exhibits a temperature coefficient of about 2.5 mv/ $^{\circ}$ C, so that for a $\pm 10^{\circ}$ C change the threshold

FIGURE 12

DISCRIMINATOR CIRCUIT DIAGRAM

ALL RESISTORS ARE GIVEN IN OHMS

VOLTAGE DISCRIMINATOR



changes by ± 25 mv. However, since the temperature coefficient is approximately the same for a given type of diode, by balancing one diode against another the net temperature coefficient does not exceed $250 \mu v/^{\circ}C$.

Thus drifts due to temperature may be reduced by an order of magnitude.

The diodes used for this purpose must also have an extremely low leakage current since leakage current is temperature dependent. Low leakage silicon type diodes (1N904) were used and the value of the bias resistor was chosen so that the change in bias is less than ± 1 mv for a $\pm 10^{\circ}C$ change in temperature.

The discriminator (Fig. 12) is designed to handle negative pulses up to $-4v$ high. Therefore a bias from 0 to $+4v$ is applied to pin 15. When double delay line pulses are applied at the input, pin 14 is connected to ground since there is no need to apply a base line compensator for such pulses.

Single Channel Analyser:

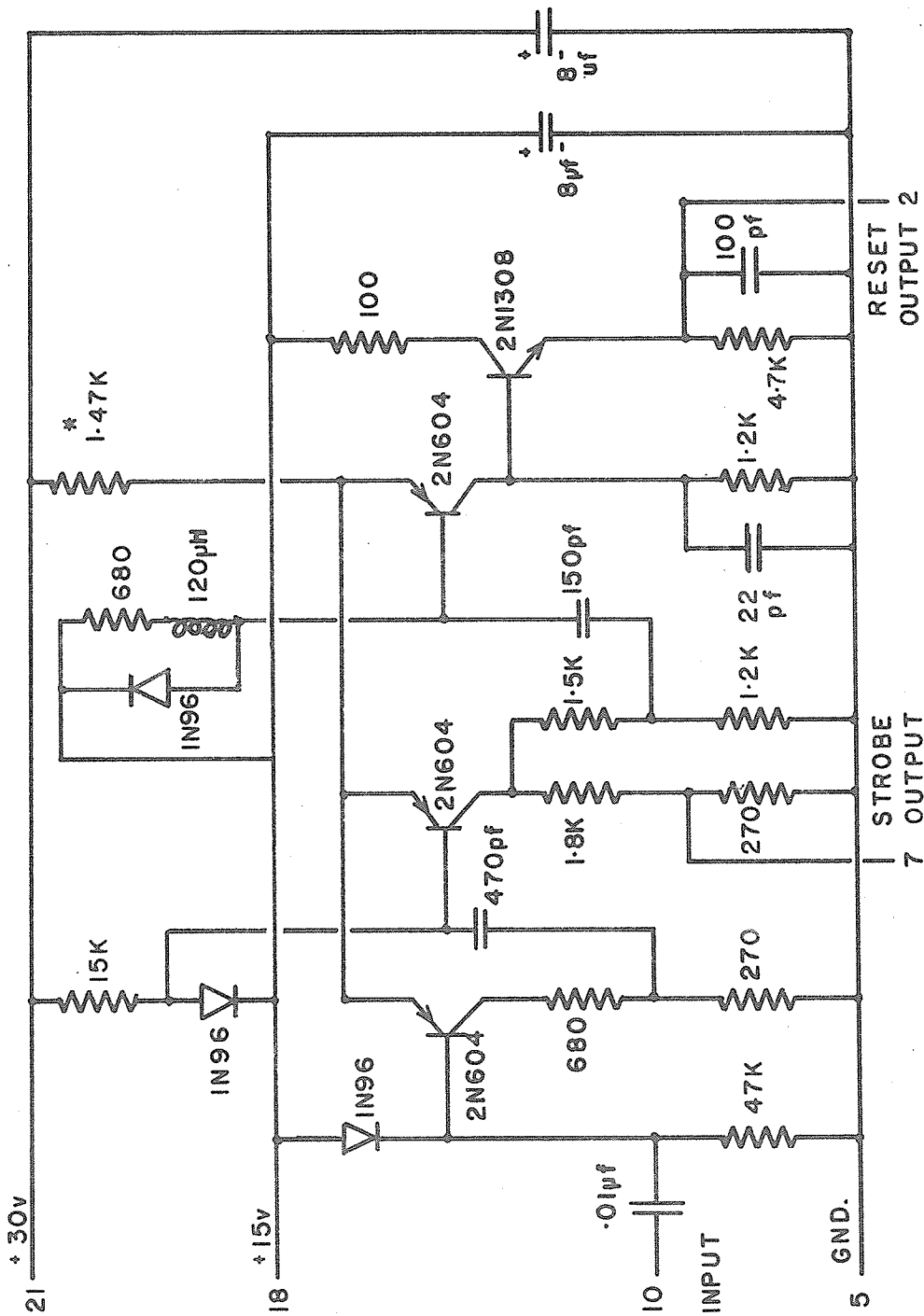
The single channel analyser consists of four units: two voltage discriminators a signal generator (strobe unit) and a slow coincidence unit. In a single channel analyser an output is desired when a pulse passes through one discriminator level but fails to pass

FIGURE 13

STROBE UNIT CIRCUIT DIAGRAM

ALL RESISTORS ARE GIVEN IN OHMS

STROBE & RESET



through another one at a higher level. This can be accomplished by putting two voltage discriminators in anticoincidence.

As the rise time of the pulses considered is not in general too fast, it is desirable to wait until the pulse is known to have passed its peak and then sample the discriminators and reset them. This sampling and resetting is achieved by means of pulses generated on the strobe board as follows. When a pulse passes through the lower discriminator level the output is fed to the strobe input. A +1v strobe pulse and a +10v reset pulse are generated, both of which are delayed with respect to the input. This guarantees that the sampling of the discriminators comes after the pulse has reached its maximum amplitude. See Fig. 13 for strobe circuit diagram.

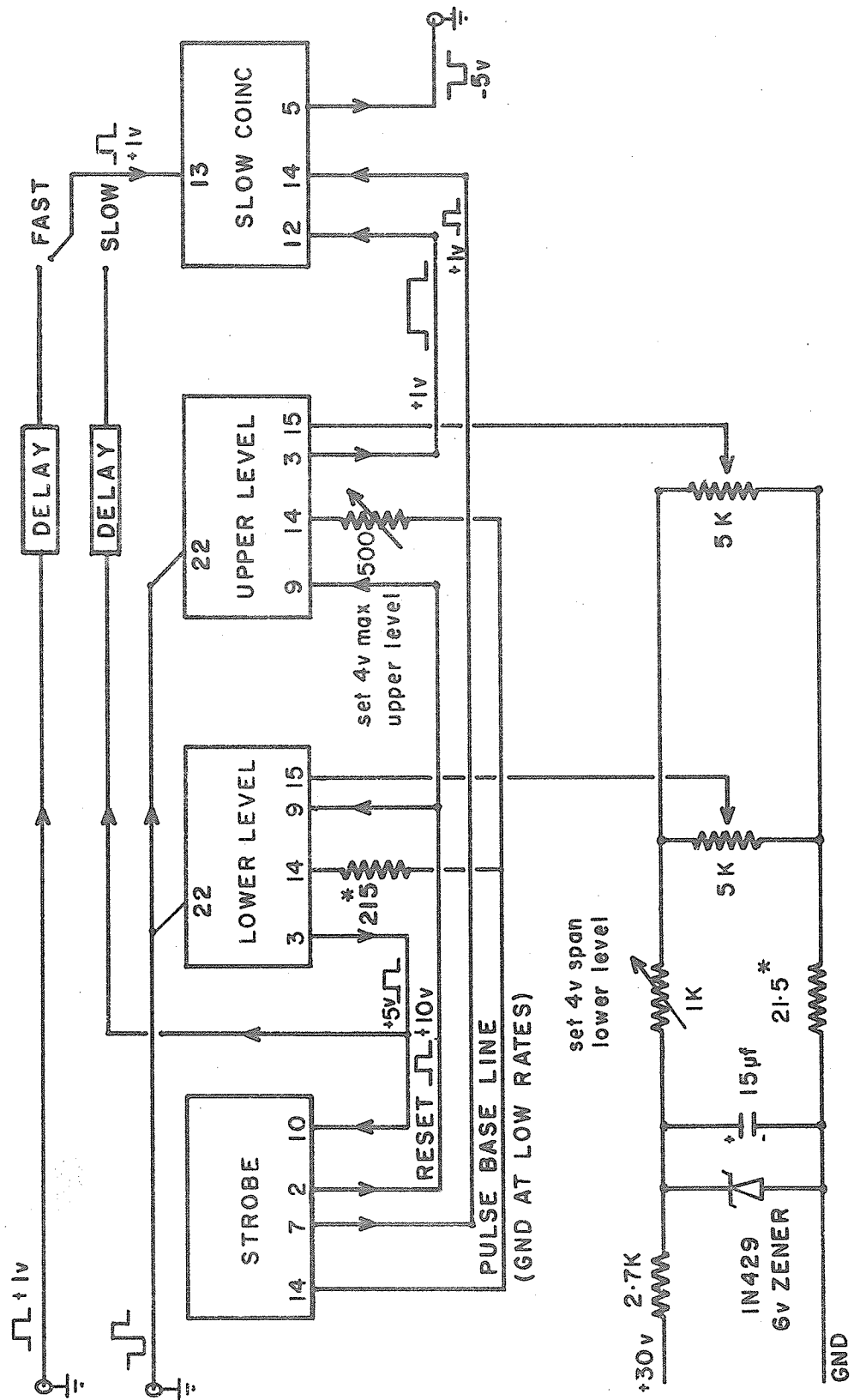
The strobe pulse is then fed to one of the coincidence inputs of the slow coincidence circuit. The output from the fast coincidence unit is fed to the other coincidence input. The anticoincidence input receives the output from the upper discriminator. This pulse must be long enough to cover the maximum possible duration of the other pulses. Thus an output from the slow coincidence unit means that two or more gamma rays were originally in coincidence and their sum was such that it passed through the lower discriminator but not through the upper.

FIGURE 14

SINGLE CHANNEL ANALYSER WIRING DIAGRAM

ALL RESISTORS ARE GIVEN IN OHMS

SINGLE CHANNEL ANALYSER



In the event that the fast coincidence unit is not desired an alternate input to the slow coincidence unit is available. The output from the lower level is delayed suitably and then fed to the input previously fed by the fast coincidence output.

The discriminator bias is developed by means of 5K HelipotS using a voltage developed across a 6V Zener reference diode. Fig. 14 is a diagram showing the biasing arrangement and the single channel analyser wiring.

The remainder of the electronic equipment used for this project was not constructed here. The multi-channel analyser used was a Tullamore Transistorized Spectrometer ST400M manufactured by The Victoreen Instrument Company, Cleveland Ohio.

The low voltage power supply used to operate the electronics was an A.E.C.L. design (by Goulding and McNaught) Model No. 1154.

Section III

RESULTS

In order to test the equipment described in the previous section of this thesis, the decays of Na^{22} and Co^{60} were studied by the sum coincidence method.

The Na^{22} decay by positron emission to the 1274 KeV excited state of Ne^{22} is followed by the emission of a 1274 KeV gamma ray to the ground state of Ne^{22} . The annihilation of the short-lived positron results in the emission of two 511 KeV gamma rays. Therefore, if a window is set at the 2.30 MeV level, a sum coincidence spectrum of these gamma rays will be observed (see Fig. 15). Peaks at 511 KeV and 1785 KeV were observed corresponding to the detection of a 511 KeV gamma ray in one crystal and the simultaneous detection of a 511 KeV and a 1274 KeV gamma ray in the other crystal.

Co^{60} decays by β^- emission to the 2.50 MeV excited state of Ni^{60} . This level de-excites by the emission of a 1.17 MeV gamma ray followed immediately by the de-excitation of the 1.33 MeV level to the ground state. Thus a sum coincidence spectrum of Co^{60} with the sum window set at 2.50 MeV should show only 1.17 MeV and 1.33 MeV gamma rays. This can be seen in Fig. 16.

FIGURE 15

Na²² SUM COINCIDENCE SPECTRUM

ALL ENERGIES ARE GIVEN IN Kev

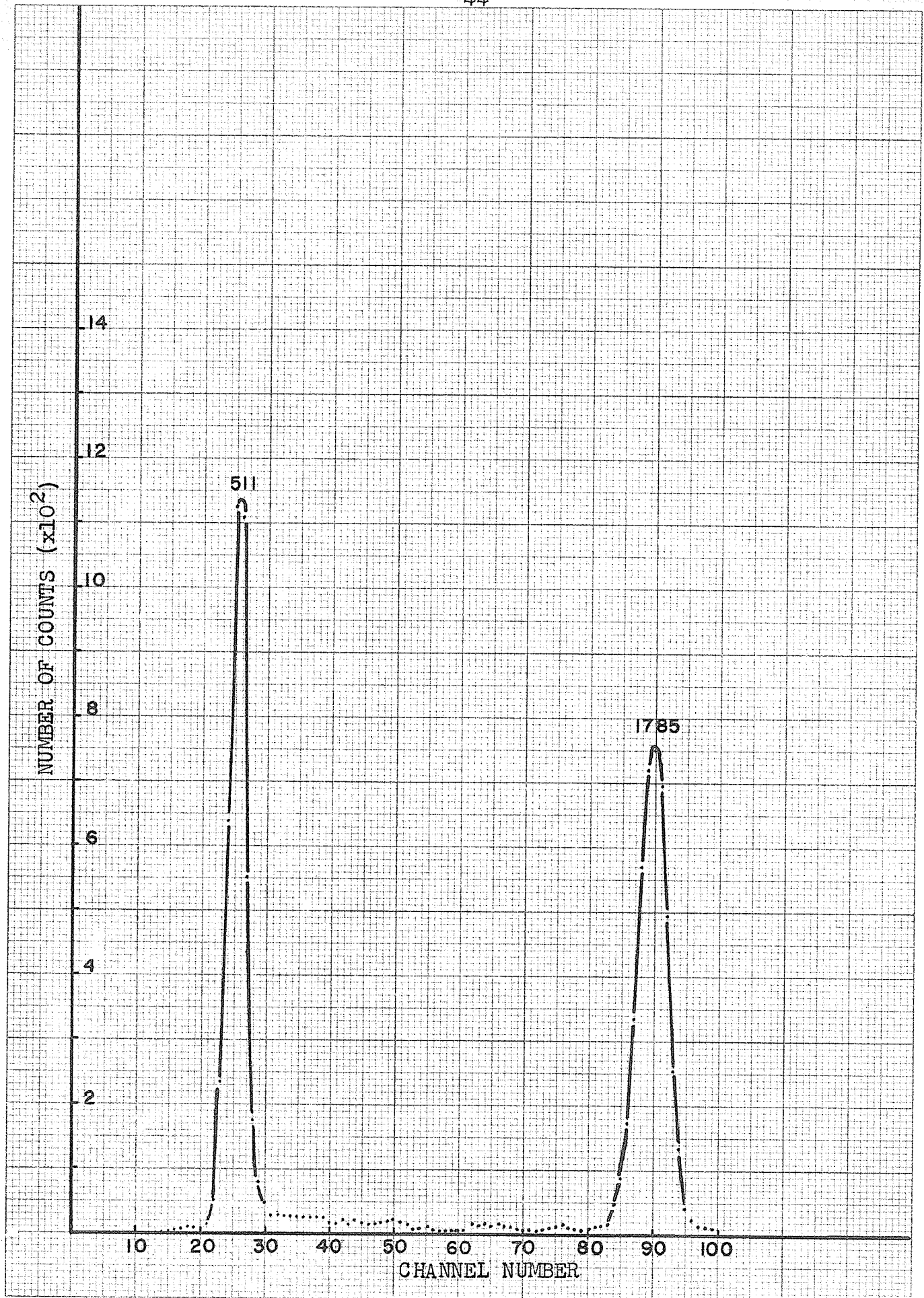
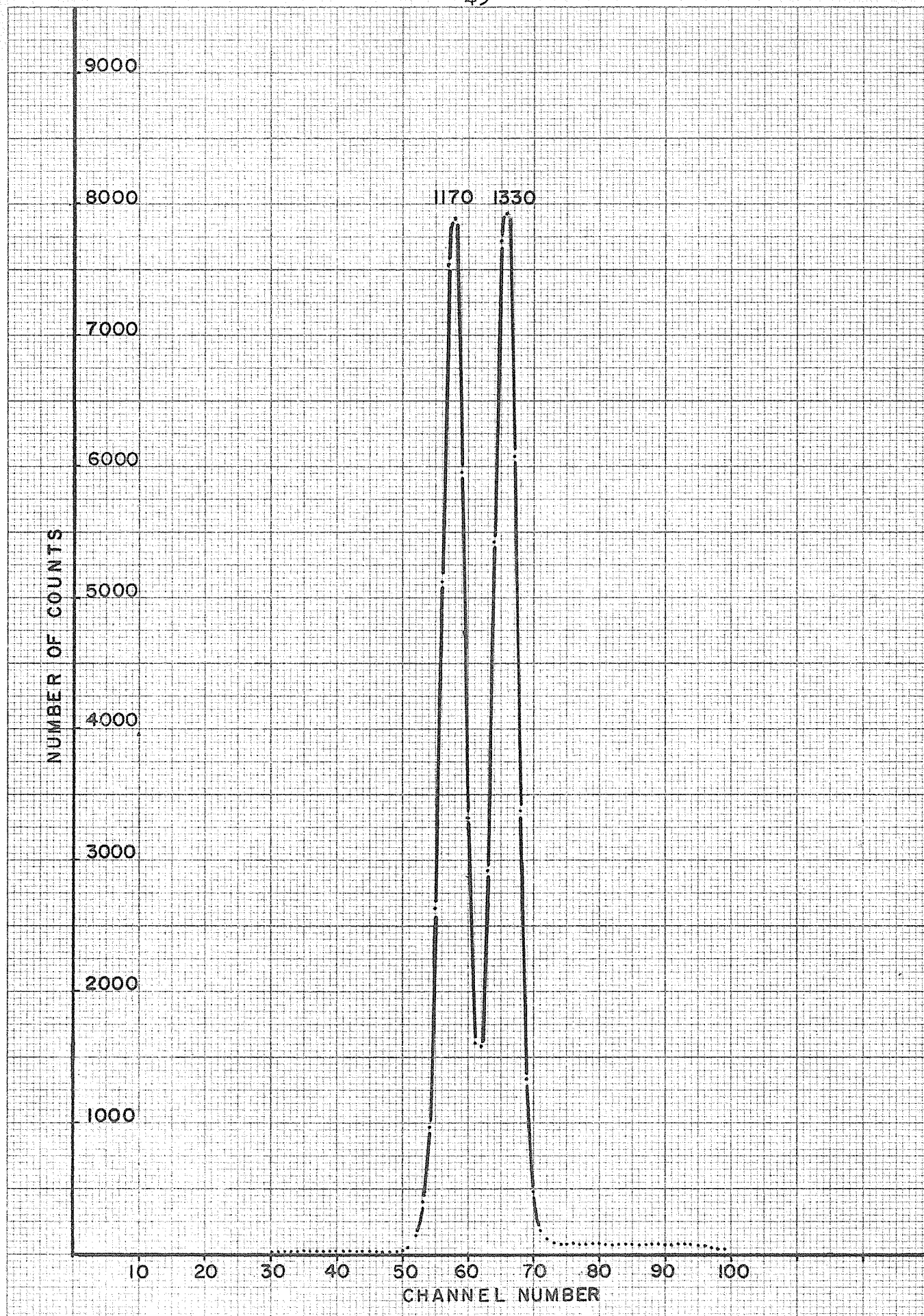


FIGURE 16

Co^{60} SUM COINCIDENCE SPECTRUM
SUM WINDOW AT 2.5 Mev
ALL ENERGIES ARE GIVEN IN Kev



It should be noted that no sum peak appears in either spectrum since the spectra were obtained using the fast coincidence mode of the spectrometer which requires one gamma ray to be detected in each crystal.

Angular Correlations

In order to check the angular correlation facilities of the sum coincidence spectrometer, an angular correlation was performed on Co^{60} .

Ni^{60} is an even-even nucleus. It is therefore particularly well suited for angular correlation studies since it has a ground state with spin 0 and even parity so the second transition must therefore be pure. The first successful directional correlation on Ni^{60} was performed by Brady & Deutsch (Brady 1947) who concluded that the gamma-gamma cascade occurred between levels with spin $4+$, $2+$ and $0+$.

The correlation function is determined experimentally by plotting the coincidence counting rate against the angle between the counters. Prior to the development of sum-coincidence spectrometer the coincidence counting rate was determined by setting single channel analysers on each of the peaks. This gives only the correlation between these two particular gamma rays. With the sum coincidence spectrometer the correlation between all the gamma ray cascades from the level under investigation can be determined at the same time.

FIGURE 17

Co^{60} ANGULAR CORRELATION CURVE

ANGLES ARE GIVEN IN DEGREES

$W(\theta)$ IN ARBITRARY UNITS

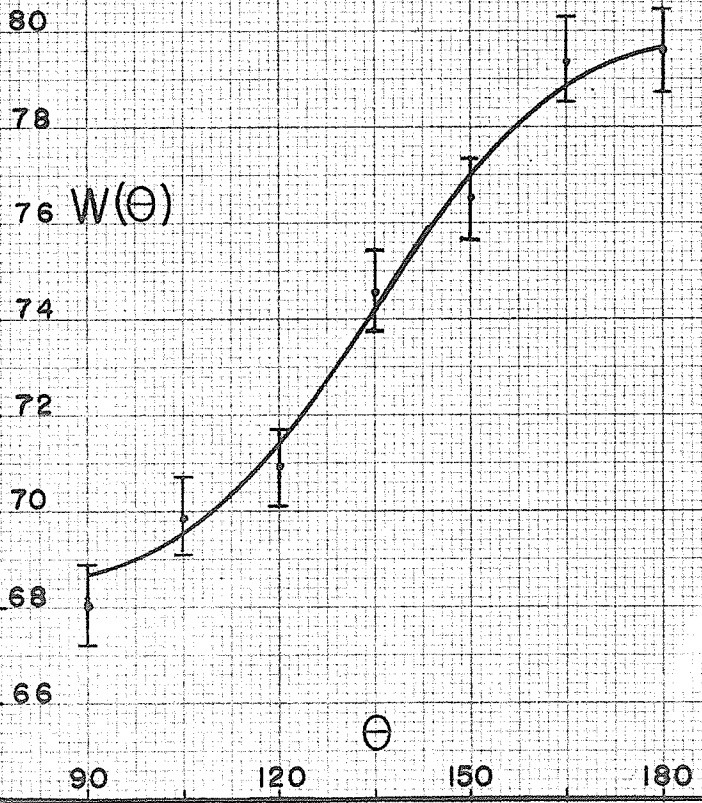
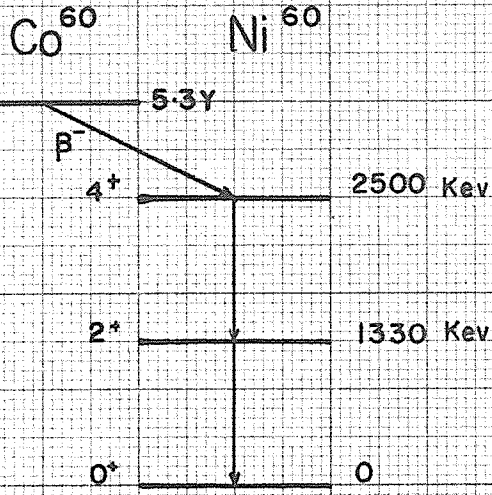


Figure 17 shows the angular correlation curve obtained by this equipment. The data were fitted to the function

$$W(\theta) = 1 + A_2 P_2(\cos \theta) + A_4 P_4(\cos \theta)$$

by a method suggested by Rose (Rose 1953). The geometrical correction for finite detector size was calculated using the method given by Feingold and Frankel (Feingold 1955).

The theoretical values of the coefficients A_2 and A_4 for the particular geometry of this experiment (crystal size 1-3/4" diameter x 2"; distance between source and detector, 10 cms) are 0.0948 and 0.007. In the experiment values of 0.104 and -0.001 were obtained. The anisotropy is theoretically 15.3% and the experimental value obtained was 16.2%

Removal of Fictitious Cascades

It is well known that a large crystal (eg. 3" x 3") has a larger photopeak to total detection efficiency than a small one (eg. 1-3/4" x 2") (Mott 1958). For a gamma ray of given energy the probability of a photoelectric interaction in a 3" x 3" crystal will be larger than that in a 1-3/4" x 2" crystal. If two spectra were obtained of a monoenergetic gamma ray source, (one with a large crystal and the other with a small one) and were normalized to the area under the photopeak, the spectrum obtained with the

large crystal would have a smaller Compton distribution than the small crystal. Conversely if the spectra were normalized to the area under the Compton distribution, the photopeak intensity in the large crystal would be greater than that in the small crystal.

Consider now a sum spectrum of Co^{60} with the sum window set at a level below 2.50 MeV. It is then possible for the photoelectric events of the 1.33 MeV gamma ray to sum with the Compton events of the 1.17 MeV gamma rays and get through the sum window. It is also possible for the photoelectric events of the 1.17 MeV gamma rays to sum with the Compton events of the 1.33 MeV gamma rays and get through the window. The possibility of Compton events of the 1.33 MeV gamma ray summing with the Compton events of the 1.17 MeV gamma ray also exists, further complicating the spectrum.

If one of the small crystals in the sum coincidence spectrometer is replaced by a large one, and the sum coincidence spectrum obtained by analysing the pulses from the large crystal, then the ratio of the areas under the peaks differs from that in the small crystal spectrum. If the spectra are normalized to the area under the 1.33 MeV photopeak, the peaks corresponding to the Compton interactions are reduced in height.

FIGURE 18

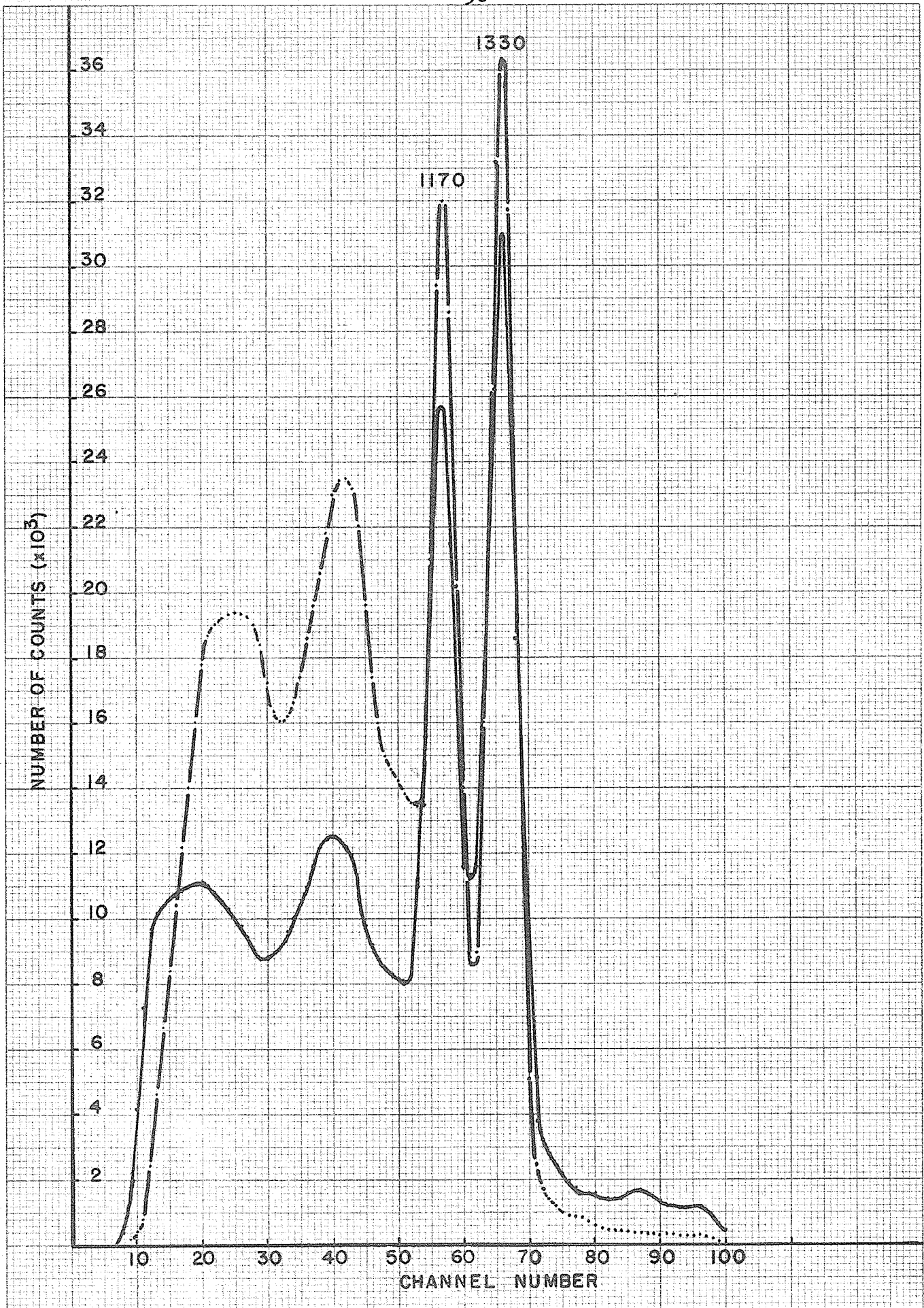
Co^{60} SUM COINCIDENCE SPECTRA

SUM WINDOW AT 1.7 Mev

ALL ENERGIES ARE GIVEN IN Kev

-o--o--o-- SMALL CRYSTAL SPECTRUM

_____ LARGE CRYSTAL SPECTRUM



Consider as an example of this technique figure 18. The sum window has its centre at channel 85. The spectrum shows clearly the photopeaks corresponding to the 1.17 MeV and 1.33 MeV gamma rays along with a broad area with two wide peaks. The spectra have been normalized to the area under the 1.33 MeV photopeak. It can be seen that the area under the lower energy peaks is larger for the case of the spectrum obtained by using two small crystals indicating that these peaks are due to Compton events rather than photoelectric events.

In an unknown decay scheme this technique, of using in turn crystals of different sizes, enables rapid identification of Compton interference to be made.

The Decay of Cs¹³⁴

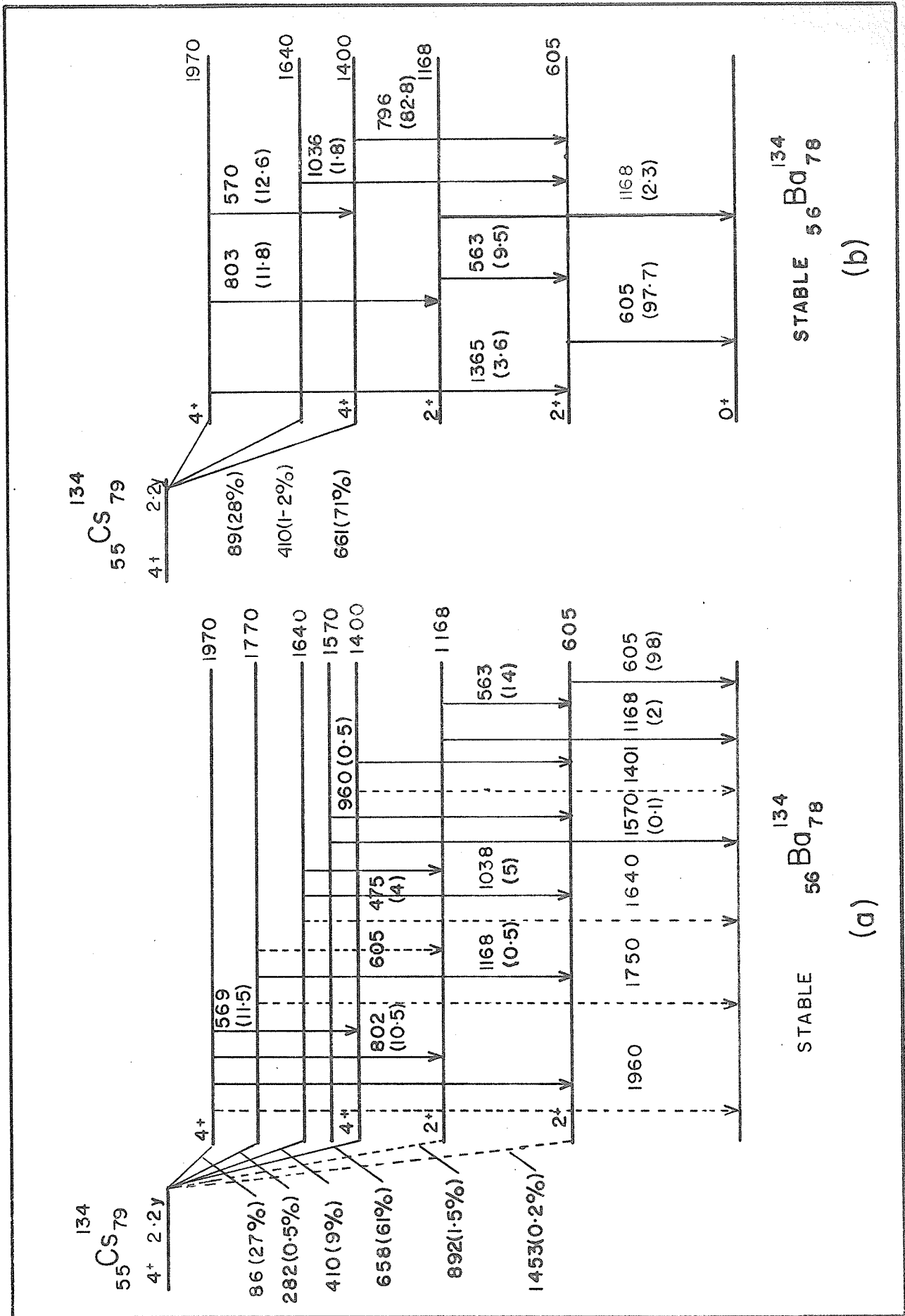
The decay of Cs¹³⁴ into Ba¹³⁴ has been the subject of much recent research (Nuclear Data Sheets). The decay scheme suggested by the Nuclear Data Sheets is shown in fig. 19a. Misinterpretation of sum coincidence spectra has resulted in the introduction of unnecessary levels into the decay scheme.

Figure 20 shows a single spectrum of Cs¹³⁴ obtained with the 3" x 3" crystal. The top level in the decay scheme has been established by several people

FIGURE 19

Cs^{134} DECAY SCHEME

- a) NUCLEAR DATA SHEETS DECAY SCHEME
- b) PROPOSED DECAY SCHEME (VANWYNGAARDEN 1964)



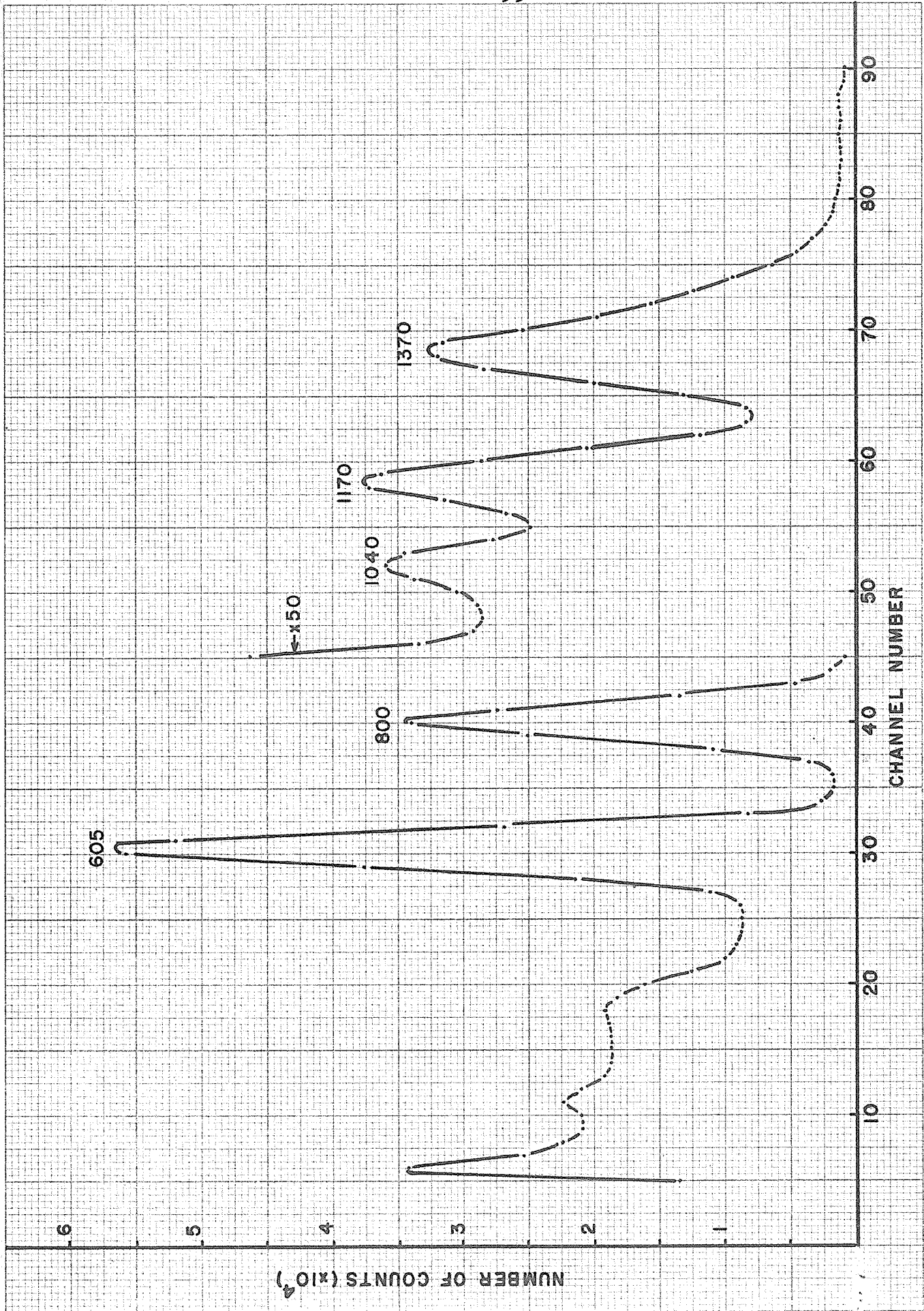
STABLE $^{134}\text{Ba}_{56}78$ (a)

STABLE $^{134}\text{Ba}_{56}78$ (b)

FIGURE 20

Cs^{134} SINGLES SPECTRUM

ALL ENERGIES ARE GIVEN IN KeV



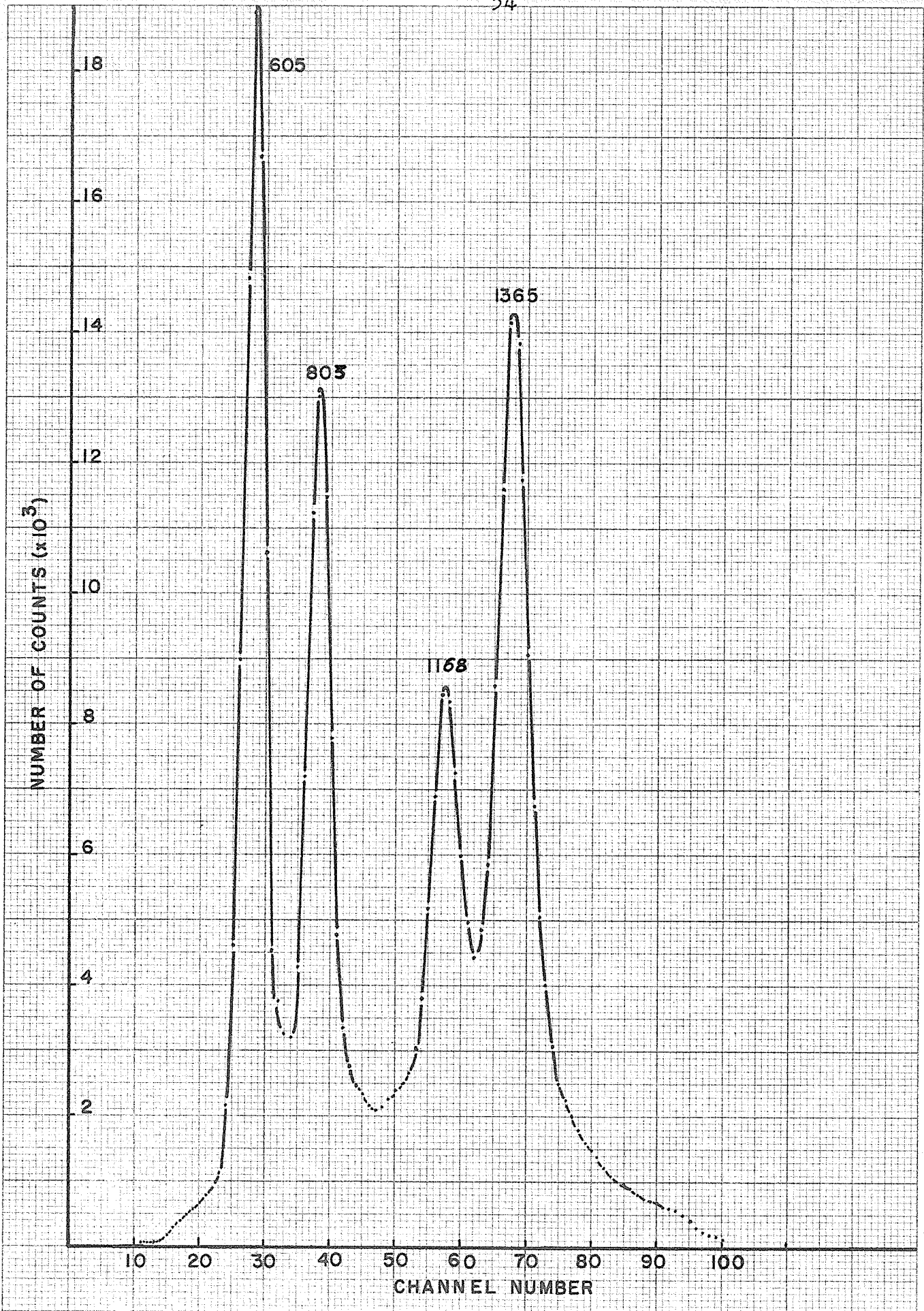


FIGURE 21

Cs^{134} SUM COINCIDENCE SPECTRUM
SUM WINDOW AT 1970 Kev
ALL ENERGIES ARE GIVEN IN Kev

(Trehan 1960, Girgis 1959, Schriber 1963) from sum coincidence spectra. As this is the uppermost level in the scheme, there can be no interference from Compton events.

Fig. 21 shows the results obtained by this experiment for the 1970 KeV level. The graph shows that there are two prominent cascades, 803 - 1168 KeV and 605 - 1365 KeV. There is, however, also the possibility of a 570 - 796 - 605 KeV cascade. The resolution of the crystals will not permit these gamma rays to be distinguished from the 605 KeV and 803 KeV gamma rays in the other two cascades. The fact that this cascade was present is shown up by the unequal areas of the 803 - 1168 KeV, and the 605 - 1365 KeV peaks. As can be seen from the graph the intensity of this cascade is much lower than either of the other two.

The benefit of the large crystal small crystal technique is demonstrated exceptionally well in the case of the 1168 KeV level. This level de-excites by the emission of a 563 KeV gamma to the 605 KeV level. There is also a lower intensity feed directly to the ground state.

The fast coincidence spectrum of this level shows three peaks. The 563 KeV and 605 KeV gammas could not be resolved with the detectors used here. The other two

FIGURE 22

Cs^{134} SUM COINCIDENCE SPECTRA

SUM WINDOW AT 1138 Kev

ALL ENERGIES ARE GIVEN IN Kev

- - - - - LARGE CRYSTAL SPECTRUM

_____ SMALL CRYSTAL SPECTRUM

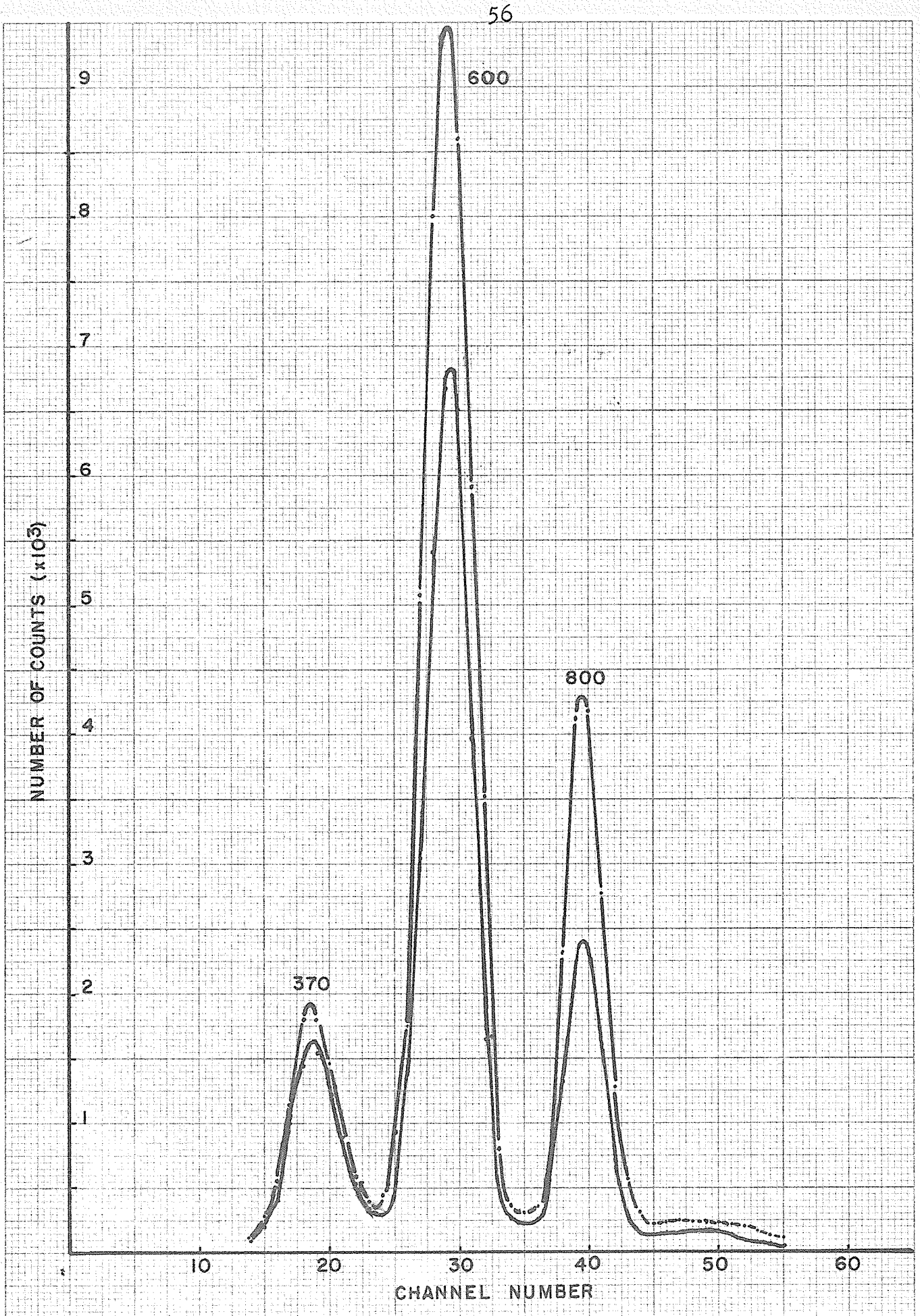


FIGURE 23

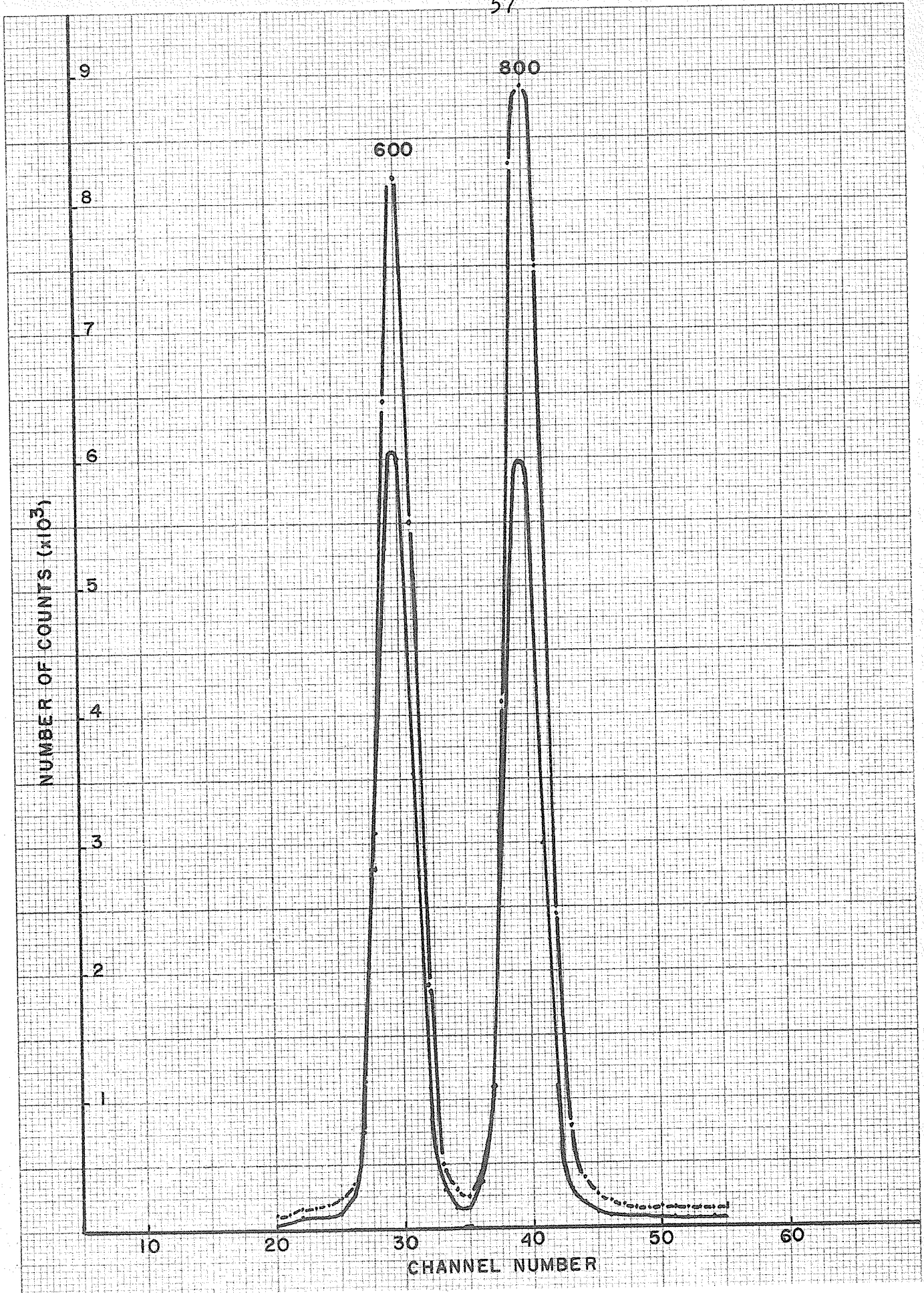
Cs^{134} SUM COINCIDENCE SPECTRA

SUM WINDOW AT 1400 Kev

ALL ENERGIES ARE GIVEN IN Kev

-.-.-.-.- LARGE CRYSTAL SPECTRUM

_____ SMALL CRYSTAL SPECTRUM



peaks are at energies of 370 KeV and 800 KeV. When the two spectra for this level are normalized to the 605 KeV area, it can be seen that, in the small crystal spectrum, the intensity of the 370 KeV peak is larger than that in the large crystal spectrum indicating that it comes from a Compton event. This means that there is not a genuine 800 - 370 KeV cascade. Presumably this is the 796 KeV gamma ray from the 1400 KeV level summing with the Compton of the 605 KeV level. The cross over transition was detected by means of the slow coincidence arrangement.

There seems to be general agreement in the literature that a level at 1400 KeV exists and that it de-excites by the emission of a 796 KeV gamma ray to be 605 KeV level. This in turn de-excites by the emission of a 605 KeV gamma ray. Figure 23 shows the results obtained in the present work with the sum window set at 1400 KeV. Only two peaks appear in the spectrum and when the large crystal spectrum is normalized to the small crystal spectrum it can be seen that they are both genuine photopeaks.

The existence of a 1640 KeV level fed by a 410 KeV beta feed of 1% intensity has also been generally agreed upon. By examining the spectra of this level (fig. 24) it seems possible that the level can decay by the following cascades: 1370 - 270 KeV, 1170 - 470 KeV, 1040 - 605 KeV and 800 - 800 KeV. However by comparing the large crystal spectrum with the small crystal spectrum it can be seen

FIGURE 24

Cs^{134} SUM COINCIDENCE SPECTRA

SUM WINDOW AT 1640 Kev

ALL ENERGIES ARE GIVEN IN Kev

-+--+-- LARGE CRYSTAL SPECTRUM

———— SMALL CRYSTAL SPECTRUM

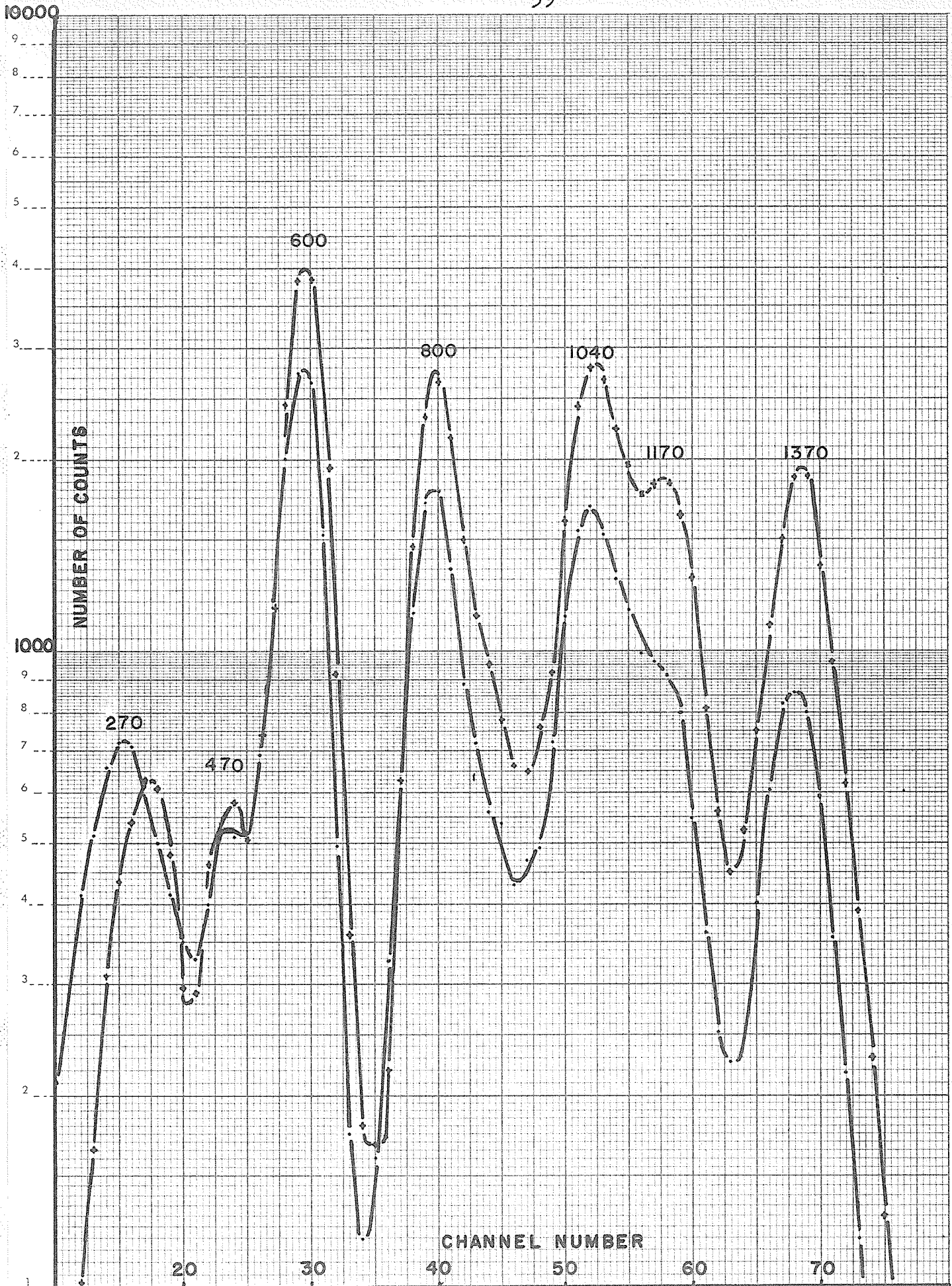


FIGURE 25

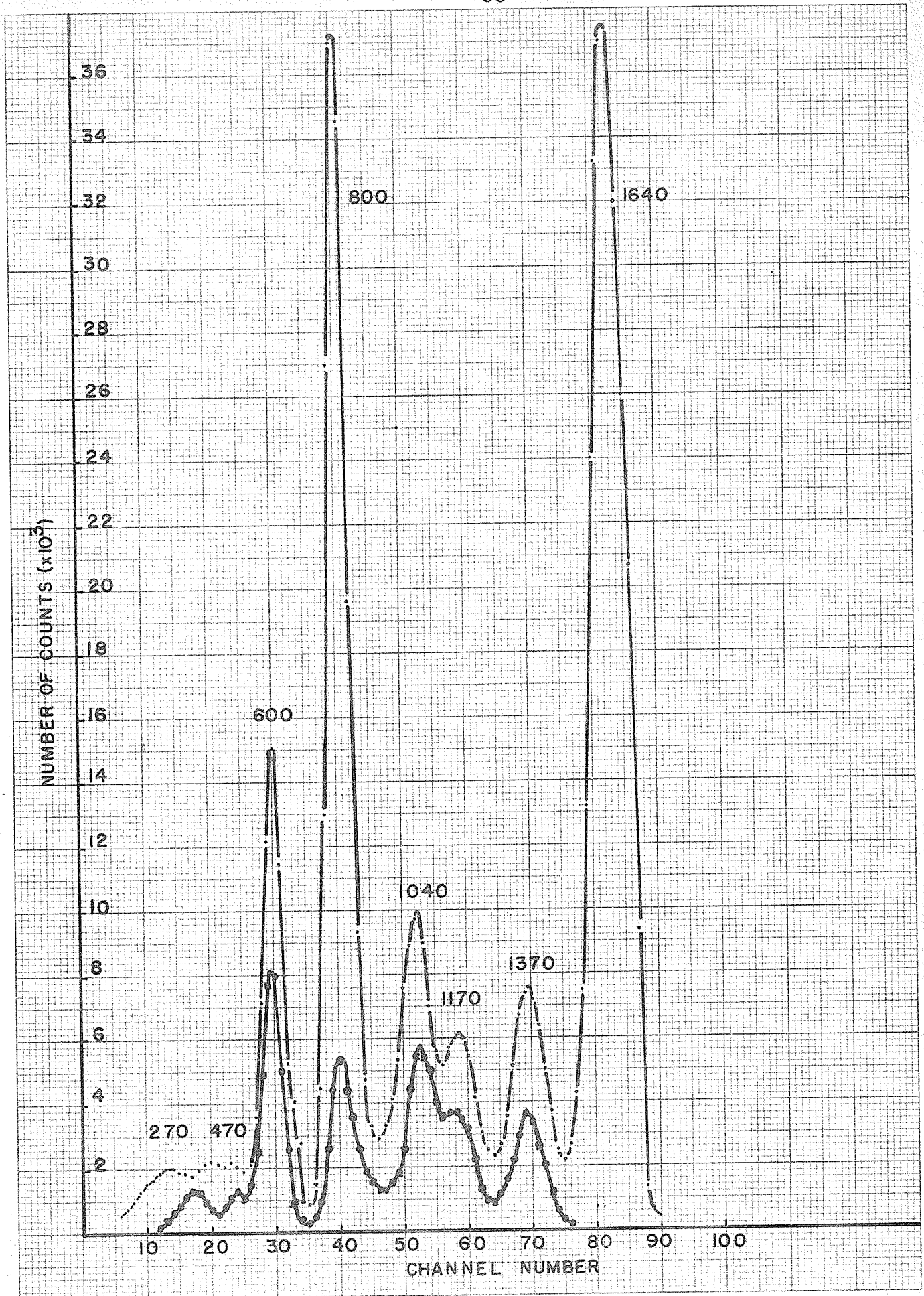
COMPARISON OF FAST AND SLOW SUM
COINCIDENCE SPECTRA

SUM WINDOW AT 1640 Kev

ALL ENERGIES ARE GIVEN IN Kev

-o'-o'-o'- SLOW COINCIDENCE SPECTRUM

_____ FAST COINCIDENCE SPECTRUM



that the 1370 - 270 cascade and the 1170 - 470 KeV cascades are fictitious. The 1040 - 600 KeV cascade however seems to be a legitimate one. The 800 - 800 KeV transition can be attributed to accidental coincidence between 800 KeV gamma rays getting through the lower edge of the sum window. That this is indeed the case can be seen by comparing the fast coincidence spectrum with the slow coincidence spectrum in figure 25. The intensity of the 800 KeV peak is much larger in the slow spectrum as would be expected with the slower resolving time. Thus it appears that the 1040 - 600 KeV transition is the true one for this level. This agrees with the results of Schriber and Hogg.

A weak level has been inserted into the scheme at 1773 KeV based on the results of sum-coincidence spectra obtained by Trehan (Trehan 1960) and Girgis (Girgis 1959) and from the 280 KeV beta feed noted by Peacock (Peacock 1957). Work carried out independently by Segaert et al. (Segaert 1963) appeared to confirm these results. However in a paper by Schriber and Hogg (Schriber 1963) a method was described for calculating and removing the peaks due to Compton interference. Their results showed that the 1773 KeV level either does not exist or its relative intensity is less than 0.2% taking the intensity of the 605 KeV level as 97.7%. A paper by VanWyngaarden and

FIGURE 26

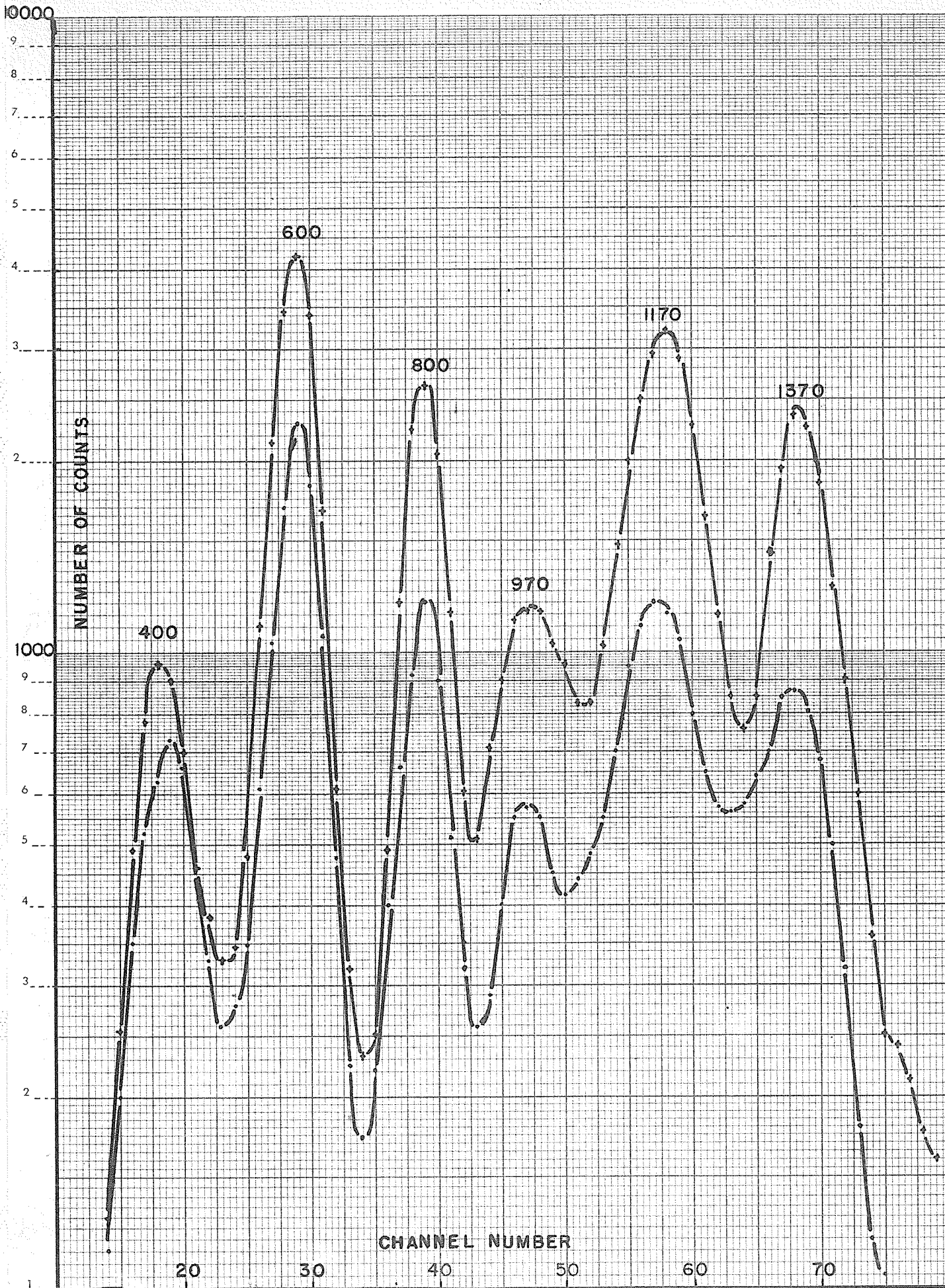
Cs^{134} SUM COINCIDENCE SPECTRA

SUM WINDOW AT 1773 Kev

ALL ENERGIES ARE GIVEN IN Kev

-+--+-- LARGE CRYSTAL SPECTRUM

-.-.-.- SMALL CRYSTAL SPECTRUM



Connor (VanWyngaarden 1964) showed no beta end point energy of 280 KeV so they omitted the 1773 KeV level from their proposed decay scheme. (See Fig. 19b.)

By examining the spectra in Fig. 26 obtained in the present work, by means of the large crystal-small crystal technique it is possible to eliminate the 400-1370 KeV and the 600-1170 KeV cascades as arising from Compton interference.

The 800-970 KeV cascade, however, appears to be a genuine one indicating that the 1773 KeV level may exist. This cascade can be accounted for without the necessity of introducing the 1773 KeV level. The 1970 KeV level de-excites by emitting an 803 KeV gamma ray to the 1168 KeV level which in turn de-excites to the ground state with the emission of an 1168 KeV gamma ray. In order to keep the geometry constant for angular correlation work, the source was surrounded by a lead shield (see figure 2) set at an angle of 45° with respect to the 180° direction. It is therefore possible for the 1168 KeV gamma ray to be scattered from this shield at a small angle ($20-30^\circ$), losing about 200 KeV in the process, and then to be detected as a full energy (photo-electric) event by the detector. Thus the large crystal-small crystal technique would fail to identify it as a Compton event.

On the basis of the present work, although it is possible to agree with the results obtained by Schriber and VanWyngaarden, the possibility of the existence of a level at 1773 KeV cannot be conclusively ruled out.

A more precise quantitative analysis of this decay scheme is required to eliminate or substantiate the existence of the 1773 KeV level.

BIBLIOGRAPHY

- Albert, R. D. - Rev. Sci. Instr. 24 (1953) 1096.
- Alder, K. - Phys. Rev. 83 (1951) 1266.
- Alder, K. - Helv. Phys. Acta 25 (1952) 235.
- Bell, P. R. - Science 120 (1954) 625.
- Bell, P. R. - "Beta and Gamma Ray Spectroscopy", Chapter 4.
Edited by K. Siegbahn. North-Holland Publishing Co. 1955.
- Birk, M., Kerns, Q. A., and Nunamaker, T. A. - University of
California Radiation Lab Report U.C.R.L. 10784.
- Biedenharn, L. C. and Rose, M. E. - Rev. Mod. Phys. 25
(1953) 729.
- Brady, E. L. and Deutsch, M. - Phys. Rev. 72 (1947) 870.
- Brady, E. L. and Deutsch, M. - Phys. Rev. 74 (1948) 1541.
- Chase, R. L. and Svelto, V. - I.R.E. Convention Record,
Part 9 (1961) 106.
- Feingold, A. M. and Frankel, S. - Phys. Rev. 97 (1955) 1025.
- Ferentz, H. and Rosenzweig, N. - Argonne National Lab Report
5324 (1954).
- Fierz, M. - Helv. Phys. Acta 22 (1949) 489.
- Fraser, J. S. and Tomlinson, R. B. - Cong. Can. Assoc. of
Physicists (1962).
- Gardner, J. W. - Proc. Phys. Soc. (London)(A) 62
(1949) 763.
- Girgis, R. K. and vanLieshout, R. - Nuc. Phys. 12 (1959) 672.
- Goertzel, G. - Phys. Rev. 70 (1946) 897.

- Goulding, F. S. and McNaught, R. A. - Nuc. Inst. and Methods 9 (1960) 282.
- Hamilton, D. R. - Phys. Rev. 58 (1940) 122.
- Hoogenboom, A. M. - Nuclear Electronics I 127 (I.A.E.A., Vienna 1959).
- Lloyd, S. P. - Phys. Rev. 80 (1950) 118.
- Lloyd, S. P. - Doctoral Thesis, University of Illinois.
- Mott, W. E. and Sutton R. B. - Handbuch der Physik 45 86 (Springer-Verlag, Berlin 1958).
- Naqvi, S. I. H. - Doctoral Thesis, University of Manitoba (1961).
- Nuclear Data Sheets - edited by Katherine Way, National Academy of Sciences, National Research Council, Washington, 1962.
- Peacock, C. L. - NP6325 (Microcard) (1957).
- Racah, G. - Phys. Rev. 84 (1951) 910.
- Rose, M. E. - Phys. Rev. 91 (1953) 610.
- Roulston, K. I. - Doctoral Thesis, University of Manitoba (1952).
- Roulston, K. I. and Naqvi, S. I. H. - Rev. Sci. Inst. 27 (1956) 830.
- Schriber, S. O. and Hogg, B. G. - Nuc. Phys. 48 (1963) 647.
- Segaert, O. J., Demuyneck, J. L., Dorikens-Vanpraet, L. V. and Dorikens, M. - Nuc. Phys. 43 (1963) 76.
- Siegbahn, K. - "Beta and Gamma Ray Spectroscopy", North-Holland Publishing Co. 1955).
- Trehan, P. N. - Doctoral Thesis, Louisiana State Univ. (1960)

VanWyngaarden, W. and Connor, R. D. - Can. J. Phys. 42

(1964) 504.

Yang, C. N. - Phys. Rev. 74 (1948) 764.